Type I immune response induces keratinocyte necroptosis and is associated with interface dermatitis

Felix Lauffer*[1], Manja Jargosch[1], Linda Krause[2], Natalie Garzorz-Stark[1], Regina Franz[1], Sophie Roenneberg[1], Alexander Böhner[1], Nikola S. Mueller[2], Fabian J. Theis[2,4], Carsten B. Schmidt-Weber[3], Tilo Biedermann[1], Stefanie Eyerich[3], Kilian Eyerich[1]

Affiliations:

[1] Department of Dermatology and Allergy, Technical University of Munich, Munich, Germany

[2] Institute of Computational Biology, Helmholtz Center Munich, Neuherberg, Germany

[3] ZAUM – Center of Allergy and Environment, Technical University and Helmholtz Center Munich, Munich, Germany

[4] Department of Mathematics, Technical University of Munich, Garching, Germany

*To whom correspondence should be addressed:

Felix Lauffer, MD

Department of Dermatology and Allergy, Technical University of Munich

Biedersteinerstraße 29, 80802 Munich, Germany

Email: felix.lauffer@tum.de

Phone: +49 89 4140 3170

Fax: +49 89 4140 3171

Short Title:

Immune response pattern of interface dermatitis

Abbreviations:

ISD: inflammatory skin disease

IFN: interferon

ID: interface dermatitis

IL: interleukin

LE: lupus erythematosus

LP: lichen planus

MLKL: mixed lineage kinase domain like pseudokinase

RIP3: receptor interacting protein kinase 3

Th: T helper

TNF: tumor necrosis factor

TCS: T cell supernatant

Abstract

Interface dermatitis (ID) is a characteristic histological pattern which occurs in autoimmune and chronic inflammatory skin diseases. It is unknown whether a common mechanism orchestrates this distinct type of skin inflammation. Here we investigated the overlap of two different ID positive skin diseases, lichen planus (LP) and lupus erythematosus (LE). The shared transcriptome signature pointed towards a strong type I immune response and biopsy derived T cells were dominated by IFN-γ and TNF-α positive cells. The transcriptome of keratinocytes stimulated with IFN-γ and TNF-α correlated significantly with the shared gene regulations of LP and LE. IFN-γ, TNF-α or mixed supernatant of lesional T cells (TCS) induced signs of keratinocyte cell death in three-dimensional skin equivalents. We detected a significantly enhanced epidermal expression of RIP3, a key regulator of necroptosis, in ID. Phosphorylation of RIP3 and MLKL was induced in keratinocytes upon stimulation with TCS; an effect which was dependent on the presence of either IFN-γ or TNF-α in the TCS. ShRNA knock-down of RIP3 prevented cell death of keratinocytes upon stimulation with IFN-γ or TNF-α. In conclusion, type I immunity is associated with LP and LE and induces keratinocyte necroptosis. These two mechanisms are potentially involved in ID.

Introduction

Inflammatory skin diseases (ISD) are a heterogeneous group of complex, immune-mediated and non-infectious skin disorders leading to disability, systemic inflammation, social stigmatization and a poor quality of life (Boehncke and Schon, 2015, Brunner et al., 2017, Eyerich et al., 2015). Over the last years, an increasing understanding of underlying immune mechanisms led to the development of specific therapeutic compounds, such as monoclonal antibodies targeting key cytokines (Noda et al., 2015). So far, research has focussed on single diseases aiming at elucidating master regulators of disease progression and, thereby, identifying new drug targets (Lauffer and Ring, 2016). Interestingly, most of the new compounds are not exclusively effective in the treatment of one ISD, but also show beneficial effects in the treatment of ISD with a similar pathogenic mechanism. Namely, monoclonal antibodies against tumour necrosis factor alpha (TNF-α) were shown to be effective in the treatment of psoriasis, hidradenitis suppurativa (acne inversa) and pityriasis rubra pilaris (Chaudhari et al., 2001, Kimball et al., 2016, Petrof et al., 2013). To exploit the full potential of available compounds, a new translational scientific approach investigating general immune response patterns of the skin in a disease independent manner is needed (Eyerich and Eyerich, 2017).

Interface dermatitis (ID), also called lichenoid tissue reaction, is a unique histological pattern which can be detected in several inflammatory and autoimmune skin diseases, such as lichen planus, lupus erythematosus, dermatomyositis, erythema multiforme, fixed drug eruption and many others. According to common definitions, ID is composed of two characteristic parts: An immune cell infiltrate close to the basal membrane of the epidermis and cell swelling and death of the undermost keratinocytes (Sontheimer, 2009). Although the initial stimulus might be different among certain skin diseases, a dominance of cytotoxic T cells and involvement of plasmacytoid dendritic cells was described in several ID positive skin diseases (Wenzel and Tuting, 2008). However, the mechanism of epidermal reaction remains poorly understood. This is reflected by a non-uniform terminology describing keratinocyte swelling as oncosis, apoptosis, necrotic degeneration or single cell necrosis. The lack of understanding ID pathogenesis is paralleled by an unmet medical need for new therapeutic targets to treat ID positive skin diseases. Thus, ID is a reasonable issue to investigate general mechanisms of skin inflammation.

The aim of this study was to investigate the underlying molecular mechanism of ID in a disease independent manner focussing on the overlap of lichen planus (LP) and lupus erythematosus (LE) in terms of histological architecture, genetic regulations and cellular immune response.

Results

The molecular signature of interface dermatitis reflects immune cell infiltration as well as epidermal reaction

Skin biopsies of LP and LE were investigated as both diseases show an ID despite their different clinical presentation (Figure 1A). In order to investigate ID specific gene regulations, whole genome expression analysis was performed in human skin biopsies of LP (n=11) and LE (n=5) in comparison to autologous healthy skin. 5675 genes were regulated exclusively in LP; 4354 genes were regulated exclusively in LE. 3888 genes showed differential regulation in both LE and LP when compared to healthy skin (Figure 1B). Only these genes were regarded as independent of the specific diseases, LP and LE, but shared among ID diseases and included in the further analysis. Pathway enrichment of shared genes showed an activation of interferon, chemokine and T cell related pathways (Figure 1C). To get a deeper understanding of gene interactions leading to ID, we performed induced modules network analysis of the top 500 regulated genes in the overlap of LP and LE (gene list in supplementary table S4). Highly connected nodes (hub genes) could be attributed to T cell immunology (TBX21, IL12R), interferon signalling (IFN-γ, IRF1, IRF2, IRF3) and response to interferon stimulation (STAT1, NFkB, RELA, ISGF3) (Figure 1D). Considering characteristics of ID, we hypothesized that hub genes indicate a type I immune dominance of infiltrating immune cells while response to interferon signalling might correspond to the epidermal reaction pattern.

Interface dermatitis is dominated by a type I immune response

Considering the strong activation of T cell pathways in our network analysis, T cells were isolated from lesional skin biopsies for in-depth analysis. Intracellular cytokine staining revealed a high frequency of IFN-γ and TNF-α positive cells in both, LE and LP. The frequency of $CD4^+$/IFN-γ^+/TNF-α^+ was significantly higher than in psoriasis (percentage of $CD4^+$ cells: LP 64.5 ± 24.1, LE 63.1 ± 18.6, psoriasis 27.9 ± 11.2, p=0.0346 LP vs. psoriasis, p=0.0466 LE vs. psoriasis), an ISD without ID (Figure 2A and 2B). In contrast, there were no significant differences in the levels of IL-4, TNF-α and IL-17A (Figure 2C). To verify a type I immune dominance *in situ,* immunohistochemical stainings for T-bet were performed. In line with the T cell immunophenotyping, a significantly higher number of T-bet-positive

cells was observed in LE and LP than in psoriasis tissue samples (10.3 ± 4.6 vs. 2.2 ± 1.2; p=0.0002) (Figure 2D).

The molecular signature of interface dermatitis resembles keratinocytes stimulated with IFN-γ and TNFα

We next addressed the question which T cell stimulus induces gene expression signatures in keratinocytes similar to the molecular signature of ID. We therefore stimulated primary human keratinocytes with the cytokine milieu produced by the T helper (Th) cell subsets Th1, Th2, Th17 and Th22 cells. Transcriptome analysis followed by induced network analysis revealed distinct molecular response patterns integrated into networks for each of the four cytokine combinations (Figure 3A). The network for keratinocytes stimulated with IFN-γ and TNF-α, lead cytokines of Th1 cells, showed the highest similarity to the network detected in human punch biopsies as both shared highly connected nodes such as IRF1, NFkB, ISGF3 and STAT1 (Figure 1D and 3A). When comparing the shared expression profile of ID to the top 100 most differentially regulated genes of keratinocytes, we detected a significant correlation with keratinocytes stimulated with IFN-γ and TNF-α, IL-17 and IL-22 as well as with IL-22 (Figure 3B). Of note, the most significant correlation was evident upon IFN-γ and TNF-α stimulation, indicating that keratinocytes in ID are exposed to a type I immune response microenvironment. Finally, we stimulated three-dimensional skin models, mimicking keratinocyte differentiation of the human epidermis, with different T cell cytokine combinations. Though this *in vitro* model is limited due to the lack of immune cells, we observed that only keratinocytes stimulated with IFN-γ and TNF-α were swollen and showed pyknotic nuclei as signs of cell death. (Figure 3C).

Necroptosis and apoptosis pathways are activated in interface dermatitis

Given the clear type I dominance in the cellular compartment and keratinocyte death which can be induced by type I cytokines, we next aimed at understanding the underlying mechanisms. Gene network analysis of the ID shared gene signature revealed signals of apoptosis (FASL), direct cytotoxicity (Granzyme B) and necroptosis (ISGF3 complex) for ID (Figure 1D and Figure 4A). In line with this observation, regulation of genes belonging to the apoptosis and necroptosis pathway were detectable in

the ID signature (Figure S2). Although the number of cleaved caspase 3 positive cells was higher in ID than in psoriasis, the majority of keratinocytes in LP and LE was negative for this marker of apoptosis, as detected by immunohistochemistry (Figure 4B upper panel). However, LP and LE tissue sections showed an epidermal expression of receptor-interacting-protein-kinase 3 (RIP3), a key protein of necroptosis (Figure 4B lower panel), which was significantly stronger than in psoriasis samples. In vitro, stimulation of keratinocytes with IFN-γ and TNF-α (10 ng/ml) resulted in induction of RIP3 like in ID, but not cleaved caspase 3 (Figure 4C). IFN-α (10 ng/ml) neither induced RIP3 nor cleaved caspase 3 in keratinocytes (Figure 4C). Next, we stimulated keratinocytes with mixed T cell supernatant (TCS) derived from LE and LP lesional T cells. Here, we observed that high doses of TCS induced both, RIP3 and cleaved caspase 3, whereas lower concentrations led to predominant induction of RIP3 and only a faint band of cleaved caspase 3 (Figure 4D). Phosphorylated MLKL as a downstream target of RIP3 was most prominently expressed in the absence of cleaved caspase 3, indicating a dose-dependent, dichotomous regulation of different cell death mechanisms. To test whether IFN-γ, TNF-α or the combination of both cytokines lead to the activation of necroptosis in keratinocytes, we depleted these cytokines in the TCS using biotinylated antibodies (Table S3). Stimulation of keratinocytes with IFN-γ-only depleted TCS as well as stimulation with TNF-α-only depleted TCS resulted in induction of RIP3 and pMLKL, while depletion of both cytokines prevented the activation of both, RIP3 and pMLKL (Figure 4E). As observed with recombinant cytokines (Figure 3C), TCS induced a cell swelling in three-dimensional skin equivalents. Similar to the induction of RIP3 and pMLKL this effect was induced by IFN-γ depleted TCS as well as by TNF-α depleted TCS, but not by IFN-γ and TNF-α depleted TCS (Figure 4F).

RIP3 is involved in keratinocyte cell death upon stimulation with TNF-α and IFN-γ

To test the impact of RIP3 for keratinocyte cell death, we performed a shRNA knockdown of RIP3 in primary human keratinocytes. Compared to control shRNA, knockdown of RIP3 using shRNA1 and shRNA3 led to a decreased phosphorylation of MLKL upon stimulation with IFN-γ and TNF-α (Figure 5A). Keratinocytes stimulated with IFN-γ and TNF-α (both 10ng/ml) showed significantly lower

frequencies of dead cells, when shRNA knock-down of RIP3 (using a 50:50 mix of shRNA1 and shRNA3) was performed compared to keratinocytes transduced with control shRNA (Figure 5B and C).

Discussion

A better understanding of general immune reaction patterns of the skin is a prerequisite to identify new therapeutic options for large groups of ISD. Beyond apotosis, we here define two additional mechanisms associated to interface dermatitis (ID): a type I dominant cellular immune response with the key cytokine IFN-γ and an activation of the necroptosis pathway mediated by the phosphorylation of RIP3 in keratinocytes.

We hypothesized that a common mechanism orchestrates the inflammatory pattern of ID in a disease independent manner. To test this hypothesis, we chose LP and LE as model diseases as they share ID, but are clinically distinct. However, when comparing the current knowledge of LP and LE pathogeneses, certain analogies are apparent, albeit both diseases are not understood entirely. Apart from case reports about patients with LP-LE-overlap syndromes (Komori et al., 2017, Lospinoso et al., 2013), there are several studies pointing towards a similar immune polarization. Observational studies described high numbers of cytotoxic T cells in LE and LP lesions (de Carvalho et al., 2016, Wenzel and Tuting, 2008). A dominance of type I immune cells could be detected by transcriptome analysis of LE skin lesions (Jabbari et al., 2014) and a high IFN-γ expression was measured in oral and cutaneous LP (Weber et al., 2016). Furthermore, genetic polymorphisms of IFN-γ are linked to LP susceptibility (Al-Mohaya et al., 2016). Some authors also claimed an important role for plasmacytoid dendritic cells and type I interferons in the pathogenesis of LE and LP (Wenzel et al., 2006, Wenzel et al., 2009). Of note, these data were mainly obtained in studies of LE, whereas the knowledge about LP pathogenesis is limited to small case series (Saadeh et al., 2016). Animal studies demonstrated that a lack of IFN-α inhibiting interferon-regulatory-factor-2 leads to skin inflammation, which is either described as psoriasis-like or lichenoid (Arakura et al., 2007, Dutz, 2009, Hida et al., 2000). Importantly, in these models the epidermal reaction is dependent on the presence of cytotoxic T cells, indicating that T cell derived IFN-γ and not IFN-α is indispensable for ID. In line with these findings, we observed a high production of IFN-γ by lesional T cells and an enhanced number of T-bet-positive cells in both, LP and LE. In our study, only stimulation with IFN-γ or TNF-α, but not stimulation with IFN-α, activated cell death

cascades in keratinocytes, thus indicating that IFN-α might be an upstream regulator of T cell response, but not directly inducing epidermal cell death.

So far, it has been assumed that apoptosis was the mechanism leading to characteristic epidermal changes of ID. Many studies have detected pro-apoptotic and anti-apoptotic signals in single keratinocytes of ID (Bascones-Ilundain et al., 2006, Skiljevic et al., 2017, Yoneda et al., 2008). In line with these observations we detected significantly higher numbers of cleaved caspase 3 positive cells in ID than in psoriasis samples. However, regarding the typical cell morphology of apoptotic cells, there is a discrepancy to histological observations: In ID keratinocytes are vacuolated and not shrunk as it would be expected for apoptotic cells (Belizario et al., 2015, Elmore, 2007, Kroemer et al., 2009). Nevertheless, the consistent picture of ID in several ISD indicates that a regulated mechanism and not accidental necrosis orchestrates the epidermal reaction.

We could observe that IFN-γ, TNF-α and a mix of lesional TCS led to cell swelling and signs of keratinocyte death in three-dimensional skin models. As expected for an in vitro model, these histological changes do not fully resemble the natural picture of ID in humans. In humans, degeneration and vacuolar changes of keratinocytes can usually be observed in the basal layer of the epidermis and keratinocytes do not show a swelling as we detected in our model. Three-dimensional skin models are limited due to the lack of immune cells and stimulation with TCS or recombinant cytokines cannot be as fine-tuned as the cell-cell-interaction *in vivo*. We used this model, however, to study the impact of single cytokines, demonstrating that IFN-γ as well TNF-α alone induce morphological changes in three-dimensional skin equivalents. Of note, in a mouse model it has been demonstrated that desmoglein specific CD4-positive IFN-γ producing T cells are indispensable for the generation of ID (Takahashi et al., 2011). Interestingly, skin lesions which develop as a side effect of novel check-point inhibitor therapies also show an ID (Schaberg et al., 2016), thus representing an *in vivo* analogy of our observation. Check point inhibitors induce a strong production of IFN-γ producing T cells and are approved for the treatment of advanced-stage melanoma (Liakou et al., 2008).

Challenging current pathology concepts, in addition to apoptosis we detected regulation of necroptosis pathway and high epidermal expression of RIP3 in ID. Necroptosis is a regulated form of cell death with

a cascade comprising phosphorylated RIP3 and MLKL which eventually builds pores of the inner and outer cell membranes (Cai et al., 2014). Influx of extracellular liquids and destruction of the osmotic barrier is paralleled by a consecutive cell swelling and cell death, respectively (Linkermann and Green, 2014). IFN-γ and TNF-α are known inducers of necroptosis (Jorgensen et al., 2017) and RIP3 is central for generation of inflammatory reactions induced by viral infections (Xu et al., 2017).

In our study we detected RIP3 broadly in the epidermis of ID. This observation conflicts with the fact that in LP or LE not all keratinocytes die. More and more reports support the hypothesis that there is an inflammatory status of necroptosis before cell death. For instance, activation of necroptosis leads to increased aerobic respiration (Yang et al., 2018) and RIP3 deficiency is associated with an induction of DNA repair pathways (Sun et al., 2018). Once activated, necroptosis can be reversed by pro-survival signals, such as the FADD-caspase8-cFLIP complex (Dillon et al., 2012). As contra-regulations might eventually prevent cell death in LP and LE, the broad expression of RIP3 indicates that necroptosis is activated in ID, even if not all affected cells finally die. In our study RIP3 was induced in primary human keratinocytes stimulated with the supernatant of lesional T cells. Depletion of IFN-γ or TNF-α revealed that both cytokines are able to induce RIP3 in human keratinocytes. RIP3 knock-down and consecutive reduction of MLKL phosphorylation led to a significant reduction of dead cells upon stimulation with IFN-γ and TNF-α. These findings are concordant with the observation that necroptosis is a key event in toxic epidermal necrolysis (TEN), a blistering skin disease characterized by cell death of the majority of keratinocytes. In fact, TEN might be regarded as disease with maximal ID and a failure of contra-regulations (Kim et al., 2015).

Understanding general immune response patterns of the skin is crucial to detect new drug targets. Recently, the discovery of necroptosis inhibitors, which interact with either RIP3 or MLKL, has been reported (Fauster et al., 2015, Yan et al., 2017). Furthermore, AMG811, a monoclonal antibody depleting IFN-γ, was tested in a phase I trial in LE. IFN-γ associated biomarkers decreased, even if there was no clinical effect on LE skin lesions after administration of one single dose (Werth et al., 2017). Phase II studies with different dosage regimes ought to clarify if there is a beneficial effect. Based on our findings, inhibition of necroptosis or targeting the IFN-γ axis are both promising therapeutic

approaches for ID positive skin reactions. This concept is supported by the fact that B cell targeting therapies are not effective for the treatment of cutaneous LE (Vital et al., 2015) and that inhibition of T cell immunology using a Janus kinase inhibitor (Klaeschen et al., 2016) or inhibition of NFkB by fumaric acid esters have proven efficacy in first studies (Kuhn et al., 2017).

Overall, our data highlight the importance of a type I cellular immune response and the suggest a role of necroptosis in the pathogenesis of ID. Given the possibility of precisely targeting the aforementioned cascades, our data warrant future translational approaches using new compounds for ID positive ISD.

Material and Methods

Patient's characteristics

34 patients with either LP (n=14), LE (n=11) or psoriasis (n=9) were enrolled in this study after obtaining written informed consent. Exclusion criteria were systemic or topical immune suppressive treatment within the last 3 months (systemic) or 1 week (topical), respectively. Patient's characteristics are listed in supplementary table 1 (Table S1). The study was approved by the local ethics committee and conducted according to ethical principles laid down in the Declaration of Helsinki.

To ensure a clear diagnosis of ID, standardized histological assessment using 24 objective and subjective criteria (Table S2) of 25 skin biopsies (LP n=14, LE n=11) was performed by two independent expert pathologists. Clustering analysis revealed a correlation of subjective ID criteria (e.g. ID subtype, ID strength) with objective criteria (the number of dyskeratotic epidermal cells, lymphocytic exocytosis; Figure S1). Given the clear relationship between the number of dyskeratotic epidermal cells and subjective rating of ID, only skin biopsies with ≥1 dyskeratotic epidermal cells were included in gene expression analysis which left eleven LP and five LE samples.

Punch biopsy specimens, histology and immunohistochemistry

6 mm punch biopsies of lesional and autologous non-lesional skin were obtained under local anaesthesia. Skin samples were fixed in 10 % formalin and embedded in paraffin. 2.5 µm sections were cut and dewaxed. After rehydration, sections were stained with haematoxylin and eosin using standard methods. For immunohistochemistry, heat induced epitope retrieval was performed in citrate buffer pH6 (Leica). Sections were incubated with the primary antibodies mouse anti-T-bet (abcam, 1:100), rabbit anti-cleaved-caspase3 (cellsignalling, 1:100) or mouse anti-RIP3 (R&D systems, 1:1000) over night at 4°C. Secondary polymeric alkaline phosphatase (AP)-linked anti-rabbit/mouse antibody or horseradish peroxidase (HRP)-linked anti-rabbit antibody (Zytomed Systems) were applied and the complex was visualized by the substrate chromogen Fast Red or 3,3'-diaminobenzidine (DAB). Eventually, slides were counterstained with haematoxylin. As a negative control, primary antibodies were omitted or

replaced with an irrelevant isotype-matched monoclonal antibody. Information about quantification of immunohistological stainings can be found in the supplementary material and methods.

Isolation of total RNA from skin biopsy and gene expression microarray

Total RNA was isolated from biopsies stored in RNA-later with the miRNeasy Mini Kit according to the manufacturer's protocol. The RNA yield and quality was determined with a Nanodrop ND1000 UV-vis Spectrophotomer. Moreover, the RNA integrity numbers (RIN) were measured using the 2100 Bioanalyzer (Agilent) according to the manufacturer's protocol (Agilent RNA 6000 Nano Kit). RNA samples with a RIN ≥ 6 were Cy3 labelled and amplified using the low input quick Amp labeling kit and hybridized on SurePrint G3 Human GE 8x60K BeadChips (Agilent Technologies). Fluorescence detection with the iScan microarray scanner and signal extraction with the Agilent Feature Extraction Software (Agilent Technologies) was used to determine specific gene expression. All microarrays were preprocessed together using the limma package in R (details in supplementary methods).

Modelling gene expression data

A detailed description about the modelling approach can be found in the supplementary methods. In short, two models were used for analyzing the human biopsy samples. One model included LP, LE and Psoriasis samples and their corresponding healthy skin samples. The second model combined LP and LE in one predictor and compared it to autologous healthy skin and psoriasis. In both models a linear mixed-effects approach was used to adjust for inter-individual variability. This results in an intercept calculated for each individual patient (= random effect) and an overall adjusted foldchange (=fixed effect) for each predictor (LE, LP, Psoriasis) compared to healthy. P-values were adjusted for multiple testing using Benjamini Hochberg (BH) correction.

Statistical analysis

Data were visualized using GraphPad Prism 7.00 software and the unpaired or paired T-test was used to test for difference in the means. Significance level was defined as $p<0.05$ (*), $p<0.01$ (**) and $p<0.001$ (***).

Induced network modules

Induced network modules of the 500 (LP and LE) or 150 (stimulated keratinocytes) top genes were calculated and displayed using *ConsensusPathDB* and *Cytoscape version 3.4.0.* software (Herwig et al., 2016, Shannon et al., 2003). Top genes are defined as significant (BH adjusted $p < 0.05$) and having the highest absolute fold change over healthy and unstimlated samples, respectively.

Pathway Analysis

We performed pathway analysis by applying the model-based gene set enrichment method *mgsa* which takes into account the hierarchical structure of pathways (Bauer S, 2016). *Wikipathways* was used as pathway resource (Kutmon et al., 2016). Pathways with an mgsa estimate larger than 0.5 are considered active.

Isolation and stimulation of lesional T cells

A detailed description about the isolation of lesional T cells can be found in the supplementary material and methods. For generation of T cell supernatant expanded lesional T cells were stimulated again with α-CD3 and α-CD28 for 72 hours. IFN-γ and TNF-α were depleted using biotinylated antibodies against IFN-γ and TNF-α (R&D systems) and streptavidin beads. Concentrations of IFN-γ and TNF-α before and after depletion were determined by ELISA (R&D systems) and are listed in Table S3. For intracellular cytokine staining, T cells were stimulated with PMA and ionomycin for 5 hours in presence of golgi inhibitors.

Lentiviral Transduction of primary human epidermal keratinocytes

Second-passage primary human epidermal keratinocytes were cultured in six-well plates and transduced with freshly concentrated lentiviral supernatant on two consecutive days. A detailed description can be found in the supplementary material and methods.

Three-dimensional skin models

Three-dimensional skin models were generated as described before (Poumay et al., 2004). A detailed description can be found in the supplementary material and methods.

Supplementary material and methods

Information on pre-processing of microarray data, modelling the gene expression data, cell culture, lentiviral vector construction, lentiviral vector production, lentiviral transduction of primary human epidermal keratinocytes, isolation of lesional T cells, three-dimensional skin models, western blot and quantification of immunohistochemical stainings can be found in the supplementary material and methods.

Acknowledgements

The authors thank Jana Sänger and Kerstin Pätzold for excellent technical support. This study was performed with samples of the biobank Biederstein of the Technical University of Munich.

Funding: This work was supported by the European Research Council (IMCIS 676858), German Research Foundation (EY97/3-1), and the Helmholtz Association ("Impuls- und Vernetzungsfonds").

Author contributions: F.L. contributed to design the project, performed experiments and wrote the manuscript; M.J., N.G. and S.E. performed experiments; L.K. performed statistical analysis and contributed to design the project; R.F., S.R. and A.B. performed histological examination; N.S.M. and F.J.T. supervised statistical analysis; C.S.W. and T.B. supervised the study design; K.E. designed and supervised the project. All authors have read and approved the final version of the manuscript.

Competing interests: The authors state no conflict of interest.

References

Al-Mohaya MA, Al-Otaibi L, Al-Harthi F, Al Bakr E, Arfin M, Al-Asmari A. Association of genetic polymorphisms in interferon-gamma, interleukin-6 and transforming growth factor-beta1 gene with oral lichen planus susceptibility. BMC oral health 2016;16(1):76.

Arakura F, Hida S, Ichikawa E, Yajima C, Nakajima S, Saida T, et al. Genetic control directed toward spontaneous IFN-alpha/IFN-beta responses and downstream IFN-gamma expression influences the pathogenesis of a murine psoriasis-like skin disease. Journal of immunology 2007;179(5):3249-57.

Bascones-Ilundain C, Gonzalez-Moles MA, Esparza-Gomez G, Gil-Montoya JA, Bascones-Martinez A. Importance of apoptotic mechanisms in inflammatory infiltrate of oral lichen planus lesions. Anticancer research 2006;26(1A):357-62.

Bauer S GJ. mgsa: Model-based gene set analysis. R package version 1.22.0. 2016.

Belizario J, Vieira-Cordeiro L, Enns S. Necroptotic Cell Death Signaling and Execution Pathway: Lessons from Knockout Mice. Mediators of inflammation 2015;2015:128076.

Boehncke WH, Schon MP. Psoriasis. Lancet 2015;386(9997):983-94.

Brunner PM, Silverberg JI, Guttman-Yassky E, Paller AS, Kabashima K, Amagai M, et al. Increasing Comorbidities Suggest that Atopic Dermatitis Is a Systemic Disorder. The Journal of investigative dermatology 2017;137(1):18-25.

Cai Z, Jitkaew S, Zhao J, Chiang HC, Choksi S, Liu J, et al. Plasma membrane translocation of trimerized MLKL protein is required for TNF-induced necroptosis. Nature cell biology 2014;16(1):55-65.

Chaudhari U, Romano P, Mulcahy LD, Dooley LT, Baker DG, Gottlieb AB. Efficacy and safety of infliximab monotherapy for plaque-type psoriasis: a randomised trial. Lancet 2001;357(9271):1842-7.

de Carvalho GC, Domingues R, de Sousa Nogueira MA, Calvielli Castelo Branco AC, Gomes Manfrere KC, Pereira NV, et al. Up-regulation of Proinflammatory Genes and Cytokines Induced by S100A8 in CD8+ T Cells in Lichen Planus. Acta dermato-venereologica 2016;96(4):485-9.

Dillon CP, Oberst A, Weinlich R, Janke LJ, Kang TB, Ben-Moshe T, et al. Survival function of the FADD-CASPASE-8-cFLIP(L) complex. Cell reports 2012;1(5):401-7.

Dutz JP. T-cell-mediated injury to keratinocytes: insights from animal models of the lichenoid tissue reaction. The Journal of investigative dermatology 2009;129(2):309-14.

Elmore S. Apoptosis: a review of programmed cell death. Toxicologic pathology 2007;35(4):495-516.

Eyerich K, Eyerich S. Immune response patterns in non-communicable inflammatory skin diseases. Journal of the European Academy of Dermatology and Venereology : JEADV 2017.

Eyerich K, Eyerich S, Biedermann T. The Multi-Modal Immune Pathogenesis of Atopic Eczema. Trends in immunology 2015;36(12):788-801.

Fauster A, Rebsamen M, Huber KV, Bigenzahn JW, Stukalov A, Lardeau CH, et al. A cellular screen identifies ponatinib and pazopanib as inhibitors of necroptosis. Cell death & disease 2015;6:e1767.

Herwig R, Hardt C, Lienhard M, Kamburov A. Analyzing and interpreting genome data at the network level with ConsensusPathDB. Nature protocols 2016;11(10):1889-907.

Hida S, Ogasawara K, Sato K, Abe M, Takayanagi H, Yokochi T, et al. CD8(+) T cell-mediated skin disease in mice lacking IRF-2, the transcriptional attenuator of interferon-alpha/beta signaling. Immunity 2000;13(5):643-55.

Jabbari A, Suarez-Farinas M, Fuentes-Duculan J, Gonzalez J, Cueto I, Franks AG, Jr., et al. Dominant Th1 and minimal Th17 skewing in discoid lupus revealed by transcriptomic comparison with psoriasis. The Journal of investigative dermatology 2014;134(1):87-95.

Jorgensen I, Rayamajhi M, Miao EA. Programmed cell death as a defence against infection. Nature reviews Immunology 2017;17(3):151-64.

Kim SK, Kim WJ, Yoon JH, Ji JH, Morgan MJ, Cho H, et al. Upregulated RIP3 Expression Potentiates MLKL Phosphorylation-Mediated Programmed Necrosis in Toxic Epidermal Necrolysis. The Journal of investigative dermatology 2015;135(8):2021-30.

Kimball AB, Okun MM, Williams DA, Gottlieb AB, Papp KA, Zouboulis CC, et al. Two Phase 3 Trials of Adalimumab for Hidradenitis Suppurativa. The New England journal of medicine 2016;375(5):422-34.

Klaeschen AS, Wolf D, Brossart P, Bieber T, Wenzel J. Beside to bench: JAK-inhibitor ruxolitinib inhibits the expression of cytokines characteristic of cutaneous lupus erythematosus. Experimental dermatology 2016.

Komori T, Otsuka A, Honda T, Kaku Y, Kabashima K. A case of chilblain lupus erythematosus with lupus erythematosus/lichen planus overlap syndrome. Journal of the European Academy of Dermatology and Venereology : JEADV 2017.

Kroemer G, Galluzzi L, Vandenabeele P, Abrams J, Alnemri ES, Baehrecke EH, et al. Classification of cell death: recommendations of the Nomenclature Committee on Cell Death 2009. Cell death and differentiation 2009;16(1):3-11.

Kuhn A, Landmann A, Bonsmann G. Fumaric acid esters: a new therapeutic option for skin manifestations in lupus erythematosus? The British journal of dermatology 2017;176(2):301-2.

Kutmon M, Riutta A, Nunes N, Hanspers K, Willighagen EL, Bohler A, et al. WikiPathways: capturing the full diversity of pathway knowledge. Nucleic acids research 2016;44(D1):D488-94.

Lauffer F, Ring J. Target-oriented therapy: Emerging drugs for atopic dermatitis. Expert opinion on emerging drugs 2016;21(1):81-9.

Liakou CI, Kamat A, Tang DN, Chen H, Sun J, Troncoso P, et al. CTLA-4 blockade increases IFNgamma-producing CD4+ICOShi cells to shift the ratio of effector to regulatory T cells in cancer patients. Proceedings of the National Academy of Sciences of the United States of America 2008;105(39):14987-92.

Linkermann A, Green DR. Necroptosis. The New England journal of medicine 2014;370(5):455-65.

Lospinoso DJ, Fernelius C, Edhegard KD, Finger DR, Arora NS. Lupus erythematosus/lichen planus overlap syndrome: successful treatment with acitretin. Lupus 2013;22(8):851-4.

Noda S, Krueger JG, Guttman-Yassky E. The translational revolution and use of biologics in patients with inflammatory skin diseases. The Journal of allergy and clinical immunology 2015;135(2):324-36.

Petrof G, Almaani N, Archer CB, Griffiths WA, Smith CH. A systematic review of the literature on the treatment of pityriasis rubra pilaris type 1 with TNF-antagonists. Journal of the European Academy of Dermatology and Venereology : JEADV 2013;27(1):e131-5.

Poumay Y, Dupont F, Marcoux S, Leclercq-Smekens M, Herin M, Coquette A. A simple reconstructed human epidermis: preparation of the culture model and utilization in in vitro studies. Archives of dermatological research 2004;296(5):203-11.

Saadeh D, Kurban M, Abbas O. Update on the role of plasmacytoid dendritic cells in inflammatory/autoimmune skin diseases. Experimental dermatology 2016;25(6):415-21.

Schaberg KB, Novoa RA, Wakelee HA, Kim J, Cheung C, Srinivas S, et al. Immunohistochemical analysis of lichenoid reactions in patients treated with anti-PD-L1 and anti-PD-1 therapy. Journal of cutaneous pathology 2016;43(4):339-46.

Shannon P, Markiel A, Ozier O, Baliga NS, Wang JT, Ramage D, et al. Cytoscape: a software environment for integrated models of biomolecular interaction networks. Genome research 2003;13(11):2498-504.

Skiljevic D, Bonaci-Nikolic B, Brasanac D, Nikolic M. Apoptosis of keratinocytes and serum DNase I activity in patients with cutaneous lupus erythematosus: relationship with clinical and immunoserological parameters. Journal of the European Academy of Dermatology and Venereology : JEADV 2017;31(3):523-9.

Sontheimer RD. Lichenoid tissue reaction/interface dermatitis: clinical and histological perspectives. The Journal of investigative dermatology 2009;129(5):1088-99.

Sun Y, Zhai L, Ma S, Zhang C, Zhao L, Li N, et al. Down-regulation of RIP3 potentiates cisplatin chemoresistance by triggering HSP90-ERK pathway mediated DNA repair in esophageal squamous cell carcinoma. Cancer letters 2018;418:97-108.

Takahashi H, Kouno M, Nagao K, Wada N, Hata T, Nishimoto S, et al. Desmoglein 3-specific CD4+ T cells induce pemphigus vulgaris and interface dermatitis in mice. The Journal of clinical investigation 2011;121(9):3677-88.

Vital EM, Wittmann M, Edward S, Md Yusof MY, MacIver H, Pease CT, et al. Brief report: responses to rituximab suggest B cell-independent inflammation in cutaneous systemic lupus erythematosus. Arthritis & rheumatology 2015;67(6):1586-91.

Weber B, Schlapbach C, Stuck M, Simon HU, Borradori L, Beltraminelli H, et al. Distinct interferon-gamma and interleukin-9 expression in cutaneous and oral lichen planus. Journal of the European Academy of Dermatology and Venereology : JEADV 2016.

Wenzel J, Scheler M, Proelss J, Bieber T, Tuting T. Type I interferon-associated cytotoxic inflammation in lichen planus. Journal of cutaneous pathology 2006;33(10):672-8.

Wenzel J, Tuting T. An IFN-associated cytotoxic cellular immune response against viral, self-, or tumor antigens is a common pathogenetic feature in "interface dermatitis". The Journal of investigative dermatology 2008;128(10):2392-402.

Wenzel J, Zahn S, Bieber T, Tuting T. Type I interferon-associated cytotoxic inflammation in cutaneous lupus erythematosus. Archives of dermatological research 2009;301(1):83-6.

Werth VP, Fiorentino D, Sullivan BA, Boedigheimer MJ, Chiu K, Wang C, et al. Pharmacodynamics, Safety, and Clinical Efficacy of AMG 811, a Human Anti-Interferon-gamma Antibody, in Subjects with Discoid Lupus Erythematosus. Arthritis & rheumatology 2017.

Xu YL, Tang HL, Peng HR, Zhao P, Qi ZT, Wang W. RIP3 deficiency ameliorates inflammatory response in mice infected with influenza H7N9 virus infection. Oncotarget 2017;8(17):27715-24.

Yan B, Liu L, Huang S, Ren Y, Wang H, Yao Z, et al. Discovery of a new class of highly potent necroptosis inhibitors targeting the mixed lineage kinase domain-like protein. Chemical communications 2017;53(26):3637-40.

Yang Z, Wang Y, Zhang Y, He X, Zhong CQ, Ni H, et al. RIP3 targets pyruvate dehydrogenase complex to increase aerobic respiration in TNF-induced necroptosis. Nature cell biology 2018;20(2):186-97.

Yoneda K, Demitsu T, Matsuoka Y, Moriue T, Nakai K, Kusida Y, et al. Subcellular activation site of caspase-3 in apoptotic keratinocytes observed in lichenoid tissue reaction. The British journal of dermatology 2008;158(5):1166-8.

Figure legends

Fig. 1 The molecular signature of interface dermatitis. **A** Clinical picture of lichen planus (LP, upper left picture) and lupus erythematosus (LE, lower left picture). Histological picture of a representative LP demonstrating a dense lichenoid infiltration of lymphocytes and vacuolated basal keratinocytes. Scale bars indicate 50 µm **B** Transcriptome analysis of LP (n=11) and LE (n=5). Depicted is the number of regulated genes shared by both LP and LE. Only the shared genes were taken into account for further analysis. **C** Active pathways (estimate larger than 0.5) of shared interface dermatitis genes. Pathways related to type I immune responses are marked in red. **D** Induced modules network analysis of the top 500 regulated genes shared by LP and LE. Node size correlates to the number of connected nodes and edges. Nodes with ≥ 8 connections are marked in red.

Fig. 2 Interface dermatitis is mediated by a strong type I immune response. **A** Representative flow cytometry plots of lichen planus (LP), lupus erythematosus (LE), and psoriasis derived T cells. **B** Frequency of IFN-γ, TNF-α double positive cells gated on CD4-positive cells and CD8-positive cells of LP (n=6), LE (n=3), and psoriasis (n=4). **C** IFN-γ, TNF-α, IL-4 and IL-17 secretion into supernatant of biopsy derived T cells of LP, LE and psoriasis. Lesional T cells of LP and LE are displayed in one bar (interface dermatitis: ID). Red points indicate LE samples. **D** Representative immunohistochemical stainings for T-bet and number of T-bet positive cells per high power field (400x). Red points indicate LE samples. Scale bars indicate 50 µm. *$p<0.05$; **$p<0.01$, *** $p<0.001$.

Fig. 3 The molecular signature of interface dermatitis resembles keratinocytes stimulated with IFN-γ and TNFα. **A** Primary human keratinocytes were stimulated with the indicated cytokine combinations (each 50 ng/ml). Induced modules networks of top 100 regulated genes as compared to unstimulated control is displayed. Node size correlates to the number of connected nodes and edges. Nodes with ≥ 5 connections are marked in red. **B** Comparison of top 100 differentially regulated genes in stimulated keratinocytes and the shared genes of LP and LE (referred to as "interface dermatitis") based on fold changes. **C** Stimulation of 3-dimensional skin models with indicated cytokine combinations (each 50 ng/ml) for 72 hours. Scale bars indicate 50 µm.

Fig. 4 Different cell death mechanisms are activated in interface dermatitis. **A** Gene network analysis revealed upregulation of apoptosis (FASLG: Fas ligand), direct cytotoxixity (GZMB: granzyme B) and necroptosis (ISGF3: interferon stimulated gene factor 3 complex). Outtake of the network shown in Figure 1D. **B** Representative immunohistochemical stainings of interface dermatitis (LE) and psoriasis biopsies for cleaved caspase 3 and RIP3. Number of cleaved caspase 3 positive cells per high power field (400x) and mean diaminobenzidine (DAB) intensity per 0,03 mm^2 in interface dermatitis (LE: n=3, LP n=3) or psoriasis (n=6). Scale bars indicate 100 µm. **C** Primary human keratinocytes were stimulated with IFN-α (10 ng/ml) or IFN-γ + TNF-α (each 10 ng/ml). Western blot for RIP3, phosphorylated MLKL (pMLKL) and cleaved caspase 3 compared to unstimulated (US). **D** Primary human keratinocytes were stimulated with mixed lesional T cell supernatant (TCS mix) derived from LP (n=6) and LE (n=3) (as shown in Figure 2). TCS was diluted with cell culture medium as indicated. Western blot for RIP3, pMLKL and cleaved caspase 3. **E** Primary human keratinocytes were stimulated with TCS mix (1:10 diluted in cell culture medium), IFN-γ depleted TCS mix (1:10), TNF-α depleted TCS mix (1:10) and IFN-γ and TNF-α depleted TCS mix. Western blot for RIP3, pMLKL and cleaved caspase 3 **F** Stimulation of 3-dimensional skin models with TCS mix (1:10 diluted in cell culture medium), IFN-γ depleted TCS mix (1:10), TNF-α depleted TCS mix (1:10) and IFN-γ and TNF-α depleted TCS mix. Scale bars indicate 50 µm.

Fig. 5 RIP3 is involved in keratinocyte death upon stimulation with IFN-γ and TNF-α **A** Western blot for RIP3, pMLKL and cleaved caspase 3 of RIP3 shRNA (three different target sequences) and control shRNA transduced primary human keratinocytes followed by stimulation with 50 ng/ml IFN-γ and TNF-α. **B** Representative FACS staining of keratinocytes transduced with RIP3 shRNA1 and shRNA3 (ratio 50:50) or control shRNA and stimulated with IFN-γ and TNF-α (each 10ng/ml). Dead cells were stained with DAPI. **C** Proportion of DAPI-positive (dead) keratinocytes within the group of RIP3 shRNA or control sh RNA transduced cells. Each pair of dots represents an independent experiment. Difference in means was tested using paired T-test. *$p<0.05$

Supplementary Figures

Supplementary Tables

Figure 1

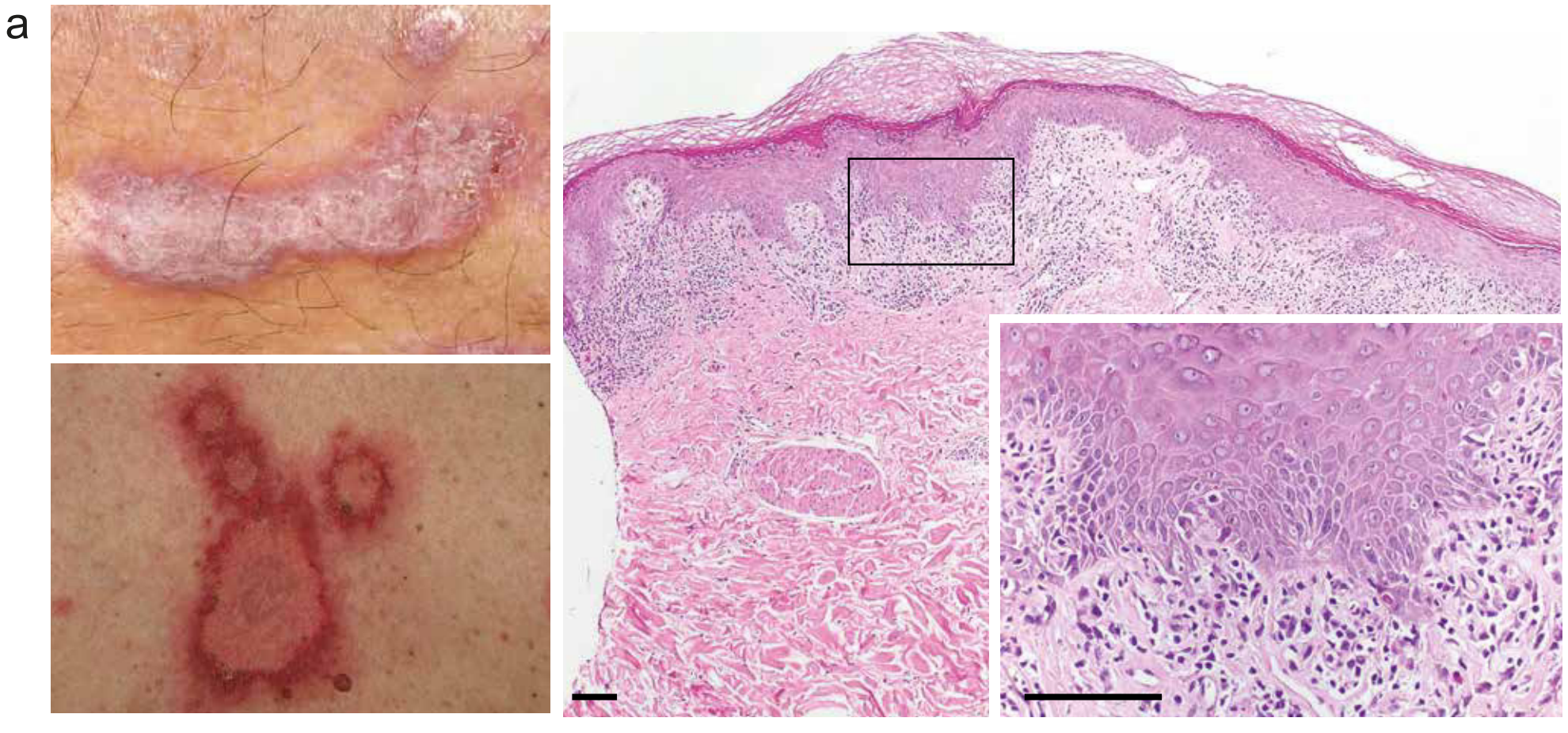
a
b
5675
3888
4354
Lupus erythematosus
Lichen planus
c
TYROBP Causal Network
Chemokine signaling pathway
RIG−I/MDA5 mediated induction of IFN−alpha/beta pathways
Interferon alpha/beta signaling
Immunoregulatory interactions between a Lymphoid and a non−Lymphoid cell
Allograft Rejection
Photodynamic therapy−induced NF−kB survival signaling
Interferon type I signaling pathways
Signaling by Interleukins
Interferon gamma signaling
Microglia Pathogen Phagocytosis Pathway
T−Cell antigen Receptor (TCR) Signaling Pathway
Fatty Acid Beta Oxidation
Eukaryotic Translation Elongation
TNFs bind their physiological receptors
Histidine, lysine, phenylalanine, tyrosine, proline and tryptophan catabolism
Wnt Signaling Pathway
Macrophage markers
Development and heterogeneity of the ILC family
Interleukin−3, 5 and GM−CSF signaling
0.00
0.25
0.50
0.75
1.00
MGSA estimate
d
CCL8
CD40LG
AKNA
CCR5
IL2RG
TRDC
TRGC1
IKZF1
ITGB2
CXCR3
CCR1
IL18RAP
BATF
LCP1
JAK3
ITGAX
CXCR4
CCL4
PLEK
CCL3
TBX21
CXCR6
IL7R
COTL1
TNFRSF9
GZMB
IDO1
IL2/IL2R
EOMES
STAT4
PDCD1
IL12/IL12R
CD19
TNFRSF4
IFNG
CCL5
IRF7
IL2RA
PAX5
PRKCQ
GZMA
IRF3
BLK
VAV1
RELA
CXCL10
RSAD2
FASLG
CCR7
IKZF3
CCL19
FOXP3
CD69
CD48
SELE
BIRC3
CXCL11
FCGR1A
MX2
SELL
CXCL1
IFIT2
MMP9
NFkB
OAS1
STAT1
ISGF3
IRF2
IRF1
IL21R
TNFSF13B
CXCL2
BCL2A1
IFIH1
MMP12
VCAM1
CXCL9
IFI27
IFI6
PSMB10
ISG20
IFIT1
CD83
IRF8
CD38
PSMB9
GBP1
ISG15
GPR18
CD74
CIITA
HLA-DRA
HLA-DMB

a

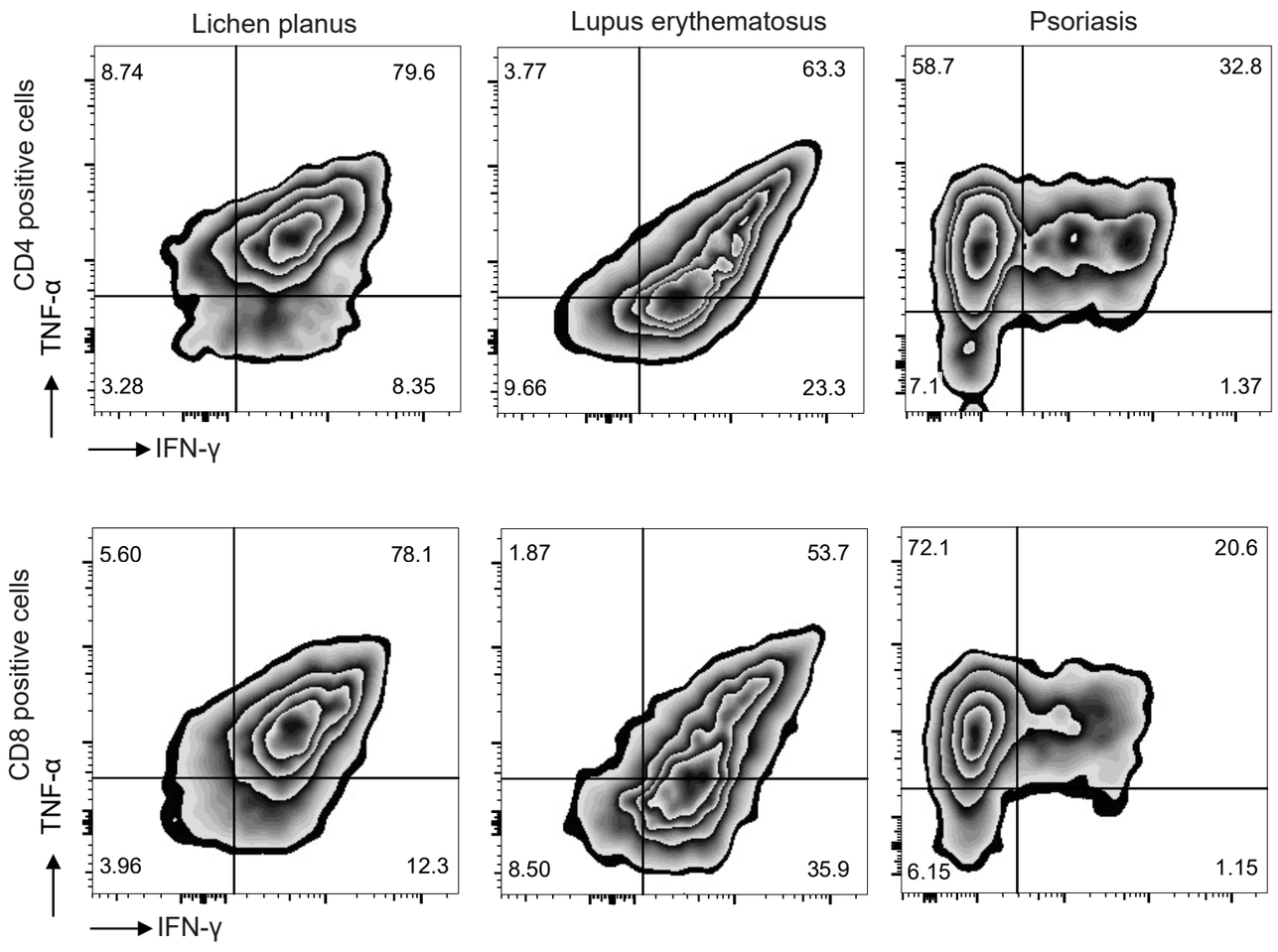
Lichen planus
Lupus erythematosus
Psoriasis
CD4 positive cells
TNF-α
IFN-γ
8.74
79.6
3.28
8.35
3.77
63.3
9.66
23.3
58.7
32.8
7.1
1.37
CD8 positive cells
TNF-α
IFN-γ
5.60
78.1
3.96
12.3
1.87
53.7
8.50
35.9
72.1
20.6
6.15
1.15

b

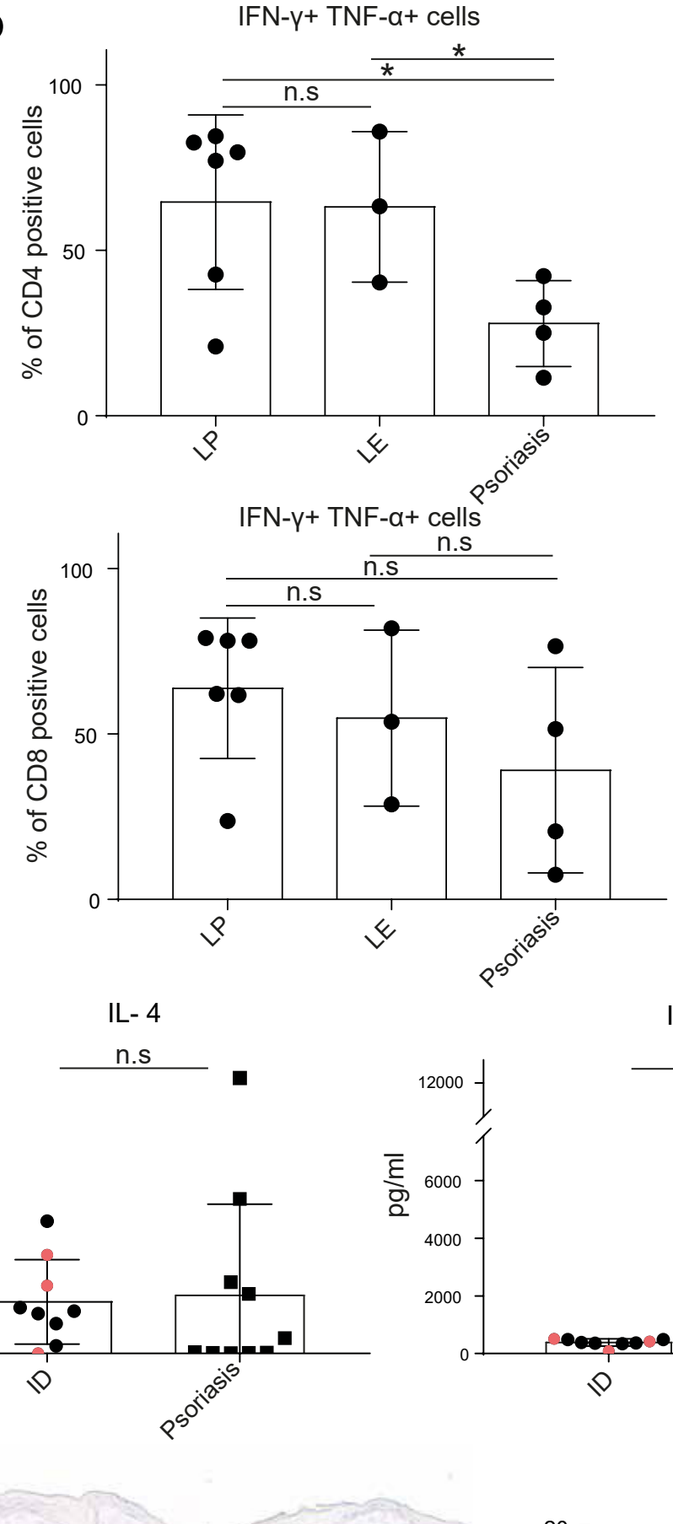
IFN-γ+ TNF-α+ cells
% of CD4 positive cells
n.s
*
*
LP
LE
Psoriasis
IFN-γ+ TNF-α+ cells
% of CD8 positive cells
n.s
n.s
n.s
LP
LE
Psoriasis

c

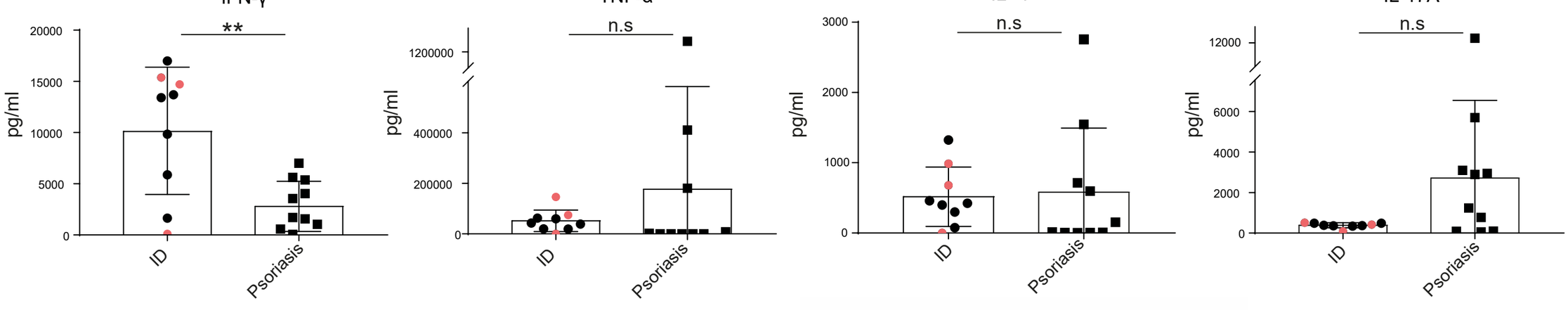
IFN-γ
pg/ml
**
ID
Psoriasis
TNF-α
pg/ml
n.s
ID
Psoriasis
IL- 4
pg/ml
n.s
ID
Psoriasis
IL-17A
pg/ml
n.s
ID
Psoriasis

d

T-bet
Lichen planus
Lupus erythematosus
Psoriasis
T-bet
number of positive cells
***
ID
Psoriasis

a

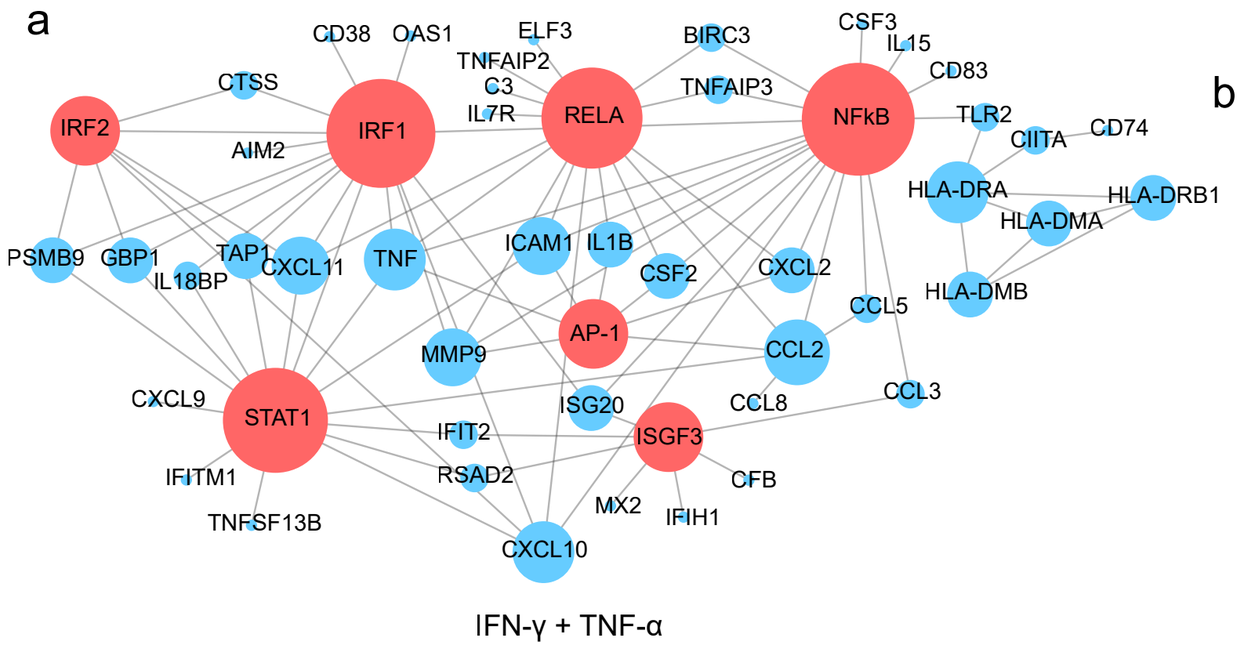

IFN-γ + TNF-α

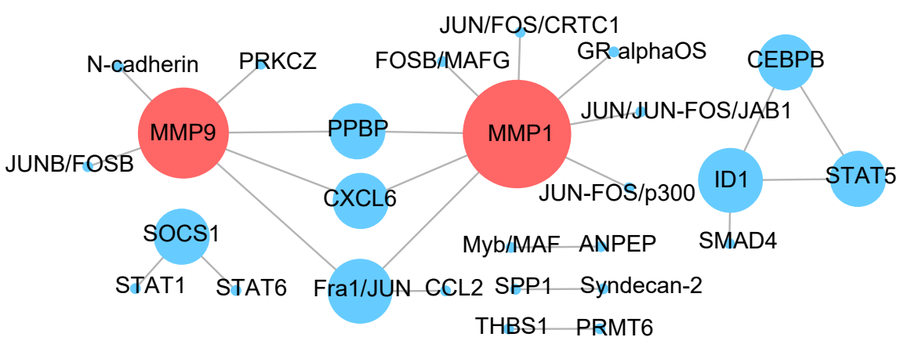

IL-4 + IL-13

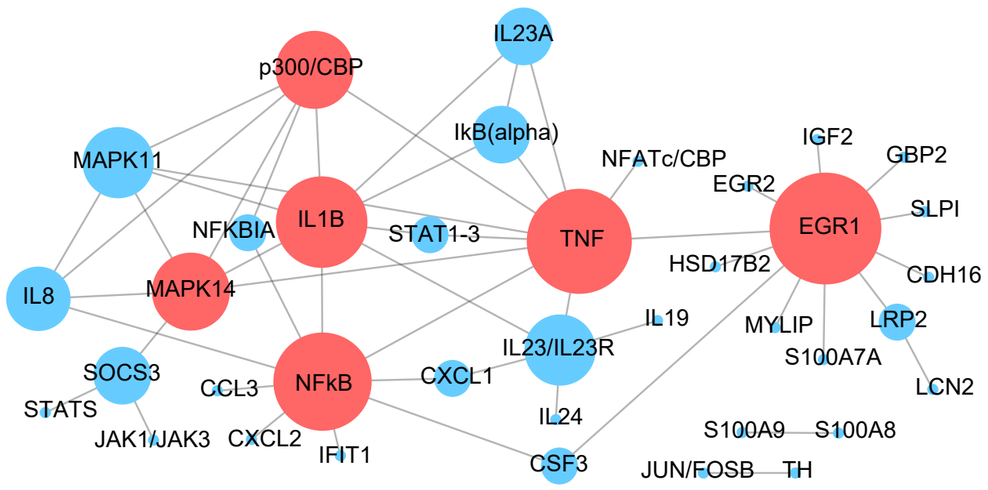

IL-17 + IL-22

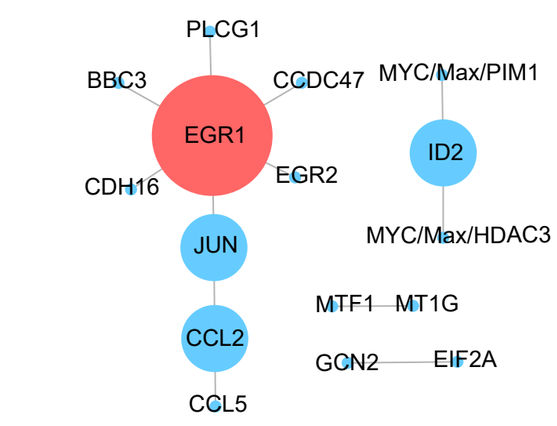

IL-22

b

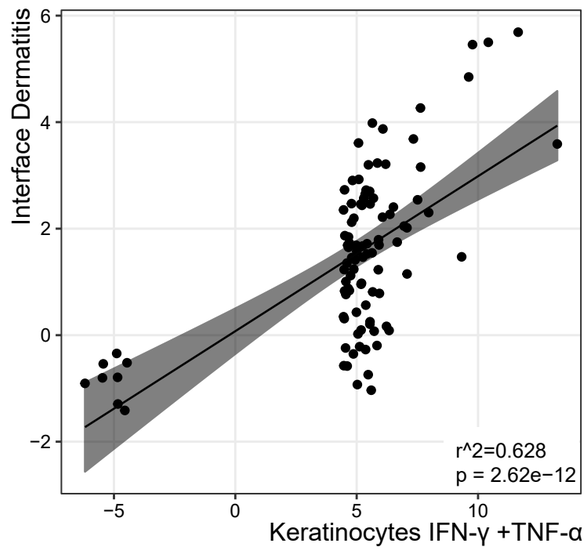

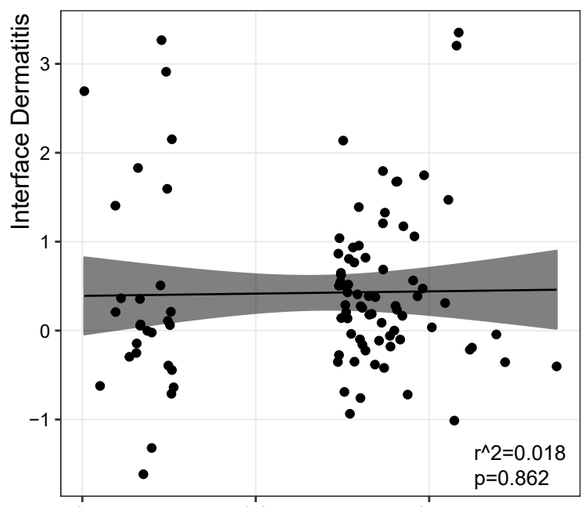

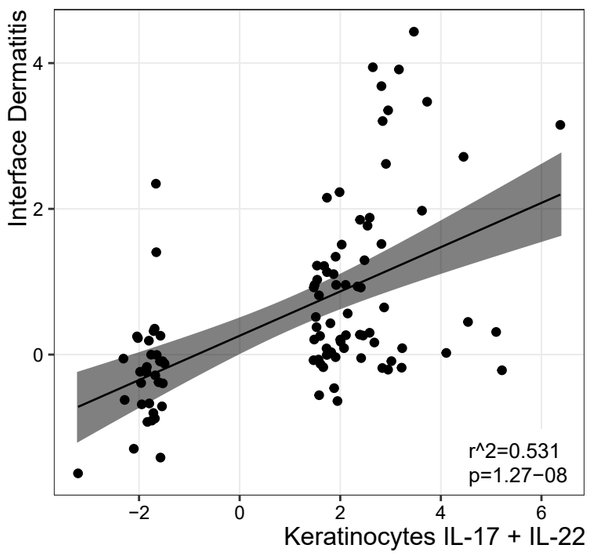

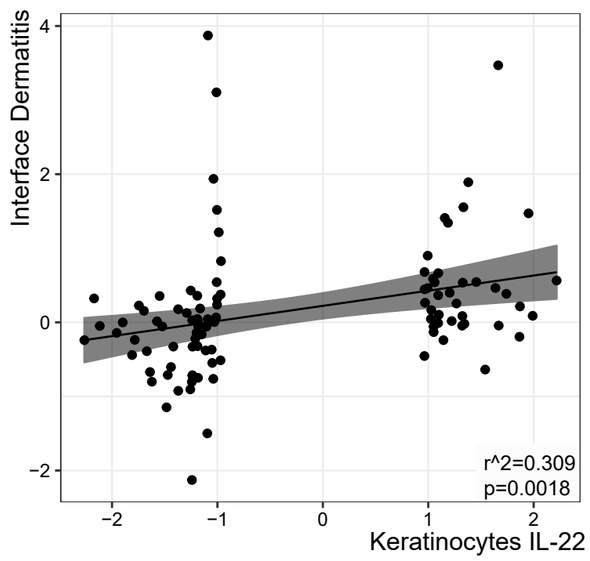

c

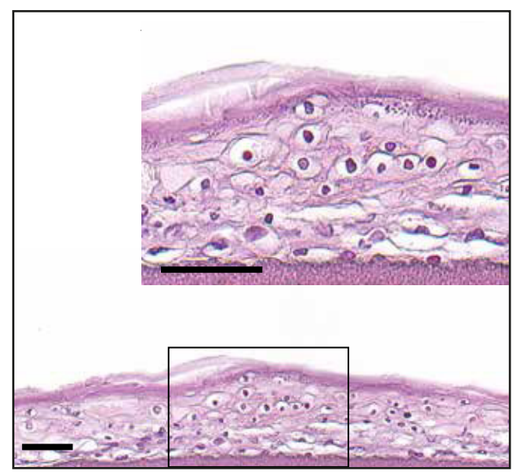

IFN-γ + TNF-α

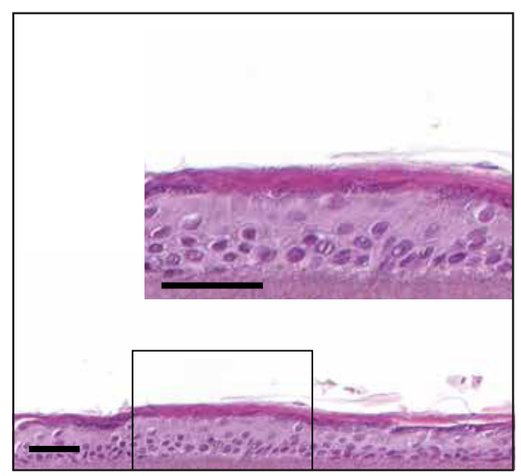

IL-4 + IL-13

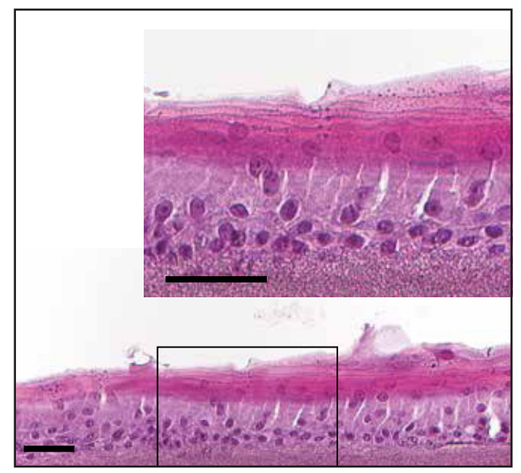

IL-17 + IL-22

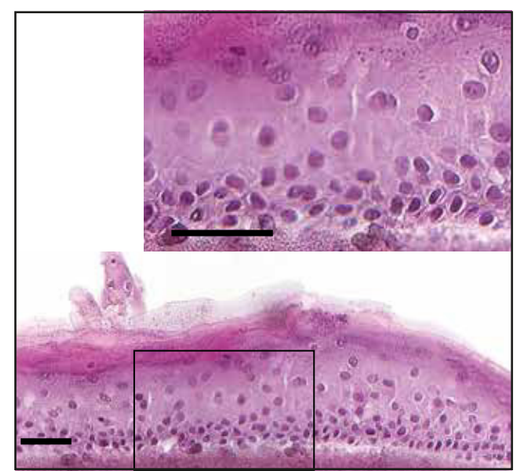

IL-22

a

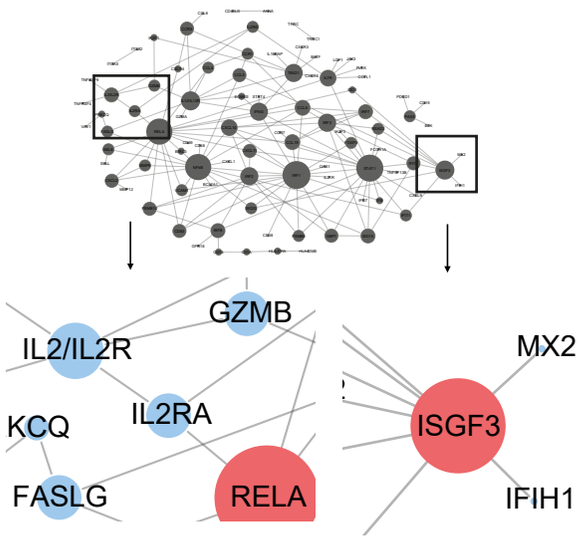
GZMB
IL2/IL2R
IL2RA
KCQ
FASLG
RELA
MX2
ISGF3
IFIH1

b

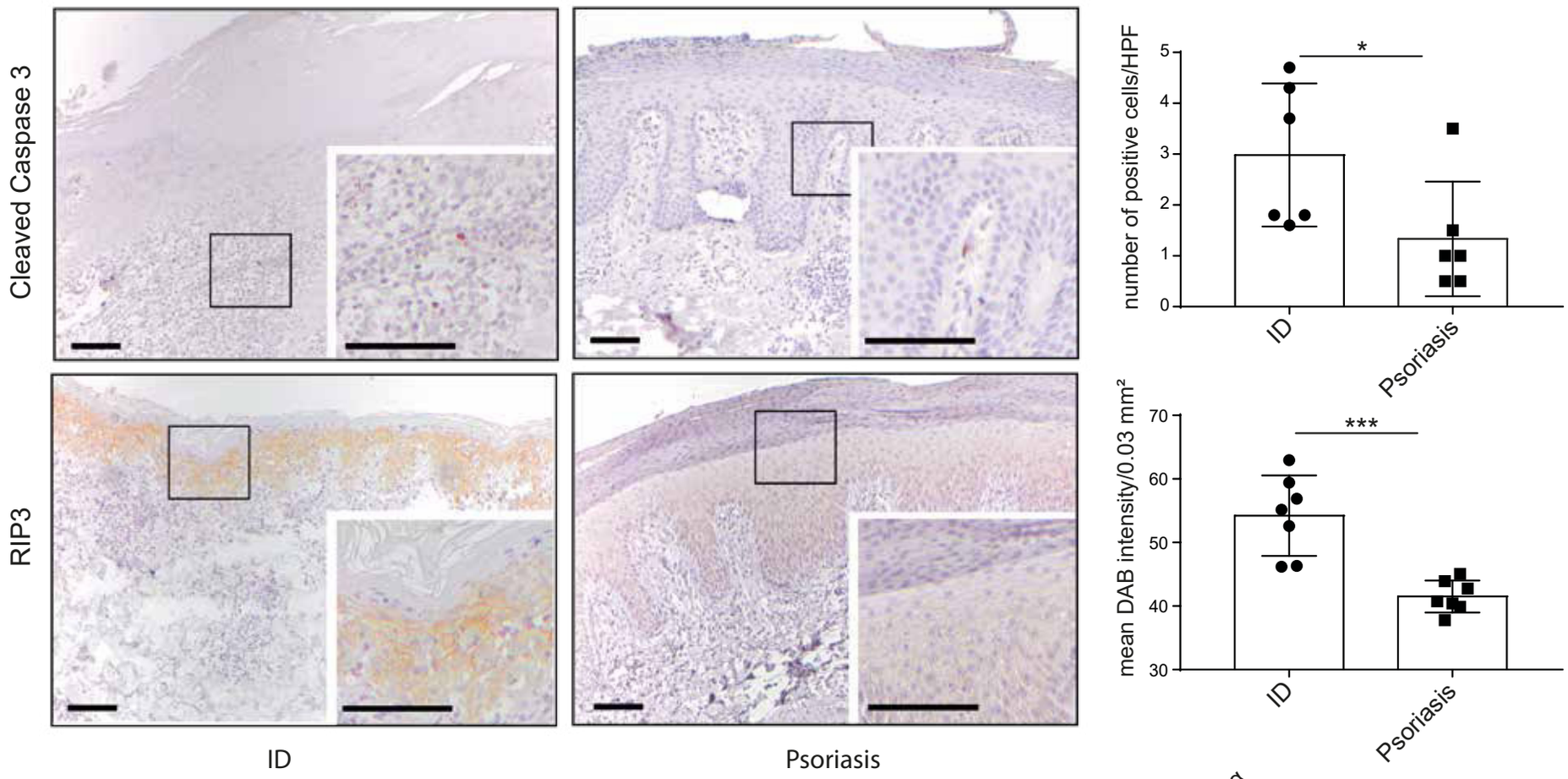
Cleaved Caspase 3
RIP3
ID
Psoriasis
number of positive cells/HPF
mean DAB intensity/0.03 mm²
*
***
ID
Psoriasis

c

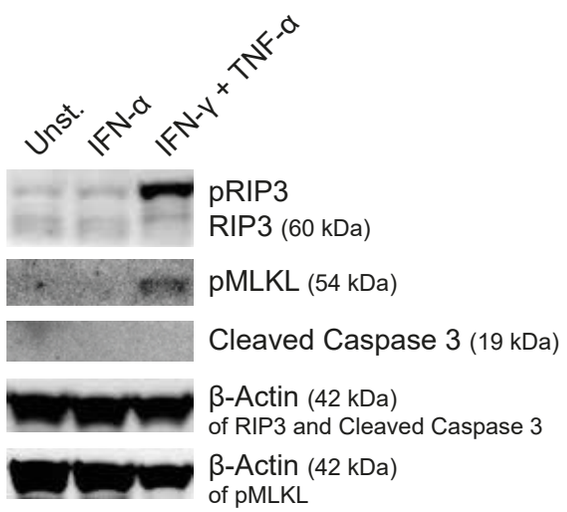
Unst.
IFN-α
IFN-γ + TNF-α
pRIP3
RIP3 (60 kDa)
pMLKL (54 kDa)
Cleaved Caspase 3 (19 kDa)
β-Actin (42 kDa)
of RIP3 and Cleaved Caspase 3
β-Actin (42 kDa)
of pMLKL

d

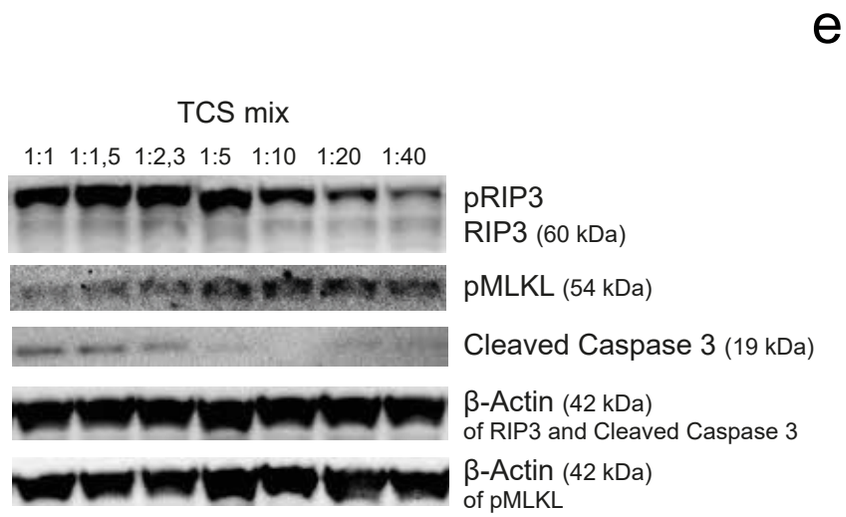
TCS mix
1:1 1:1,5 1:2,3 1:5 1:10 1:20 1:40
pRIP3
RIP3 (60 kDa)
pMLKL (54 kDa)
Cleaved Caspase 3 (19 kDa)
β-Actin (42 kDa)
of RIP3 and Cleaved Caspase 3
β-Actin (42 kDa)
of pMLKL

e

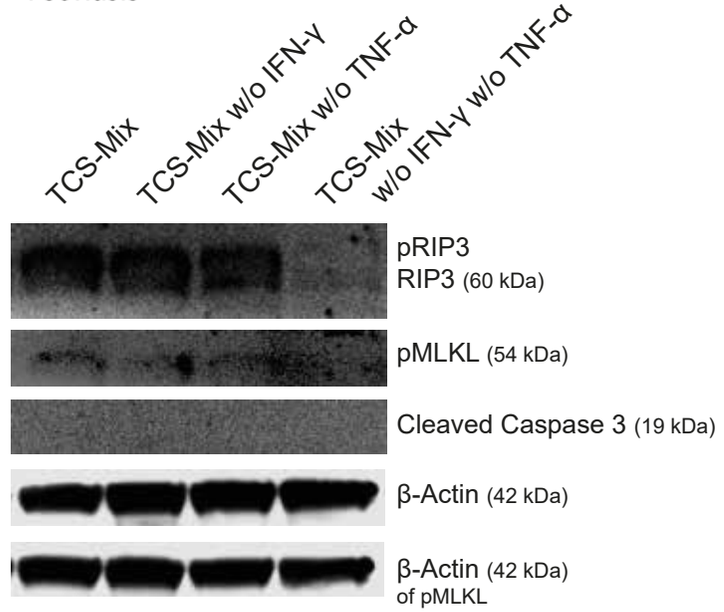
TCS-Mix
TCS-Mix w/o IFN-γ
TCS-Mix w/o TNF-α
TCS-Mix w/o IFN-γ w/o TNF-α
pRIP3
RIP3 (60 kDa)
pMLKL (54 kDa)
Cleaved Caspase 3 (19 kDa)
β-Actin (42 kDa)
β-Actin (42 kDa)
of pMLKL

f

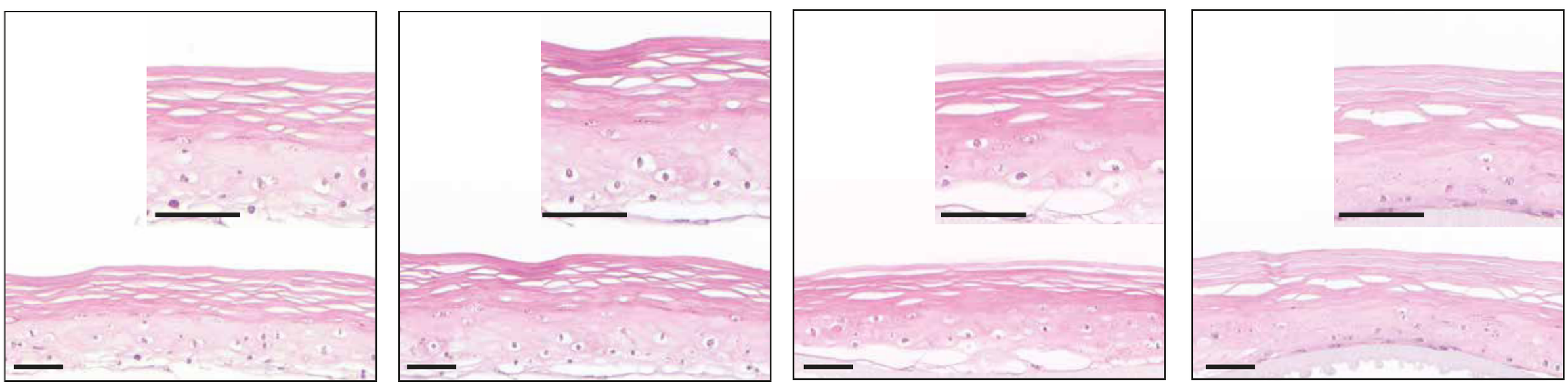
TCS Mix
TCS Mix w/o IFN
TCS Mix w/o TNF
TCS Mix w/o IFN w/o TNF

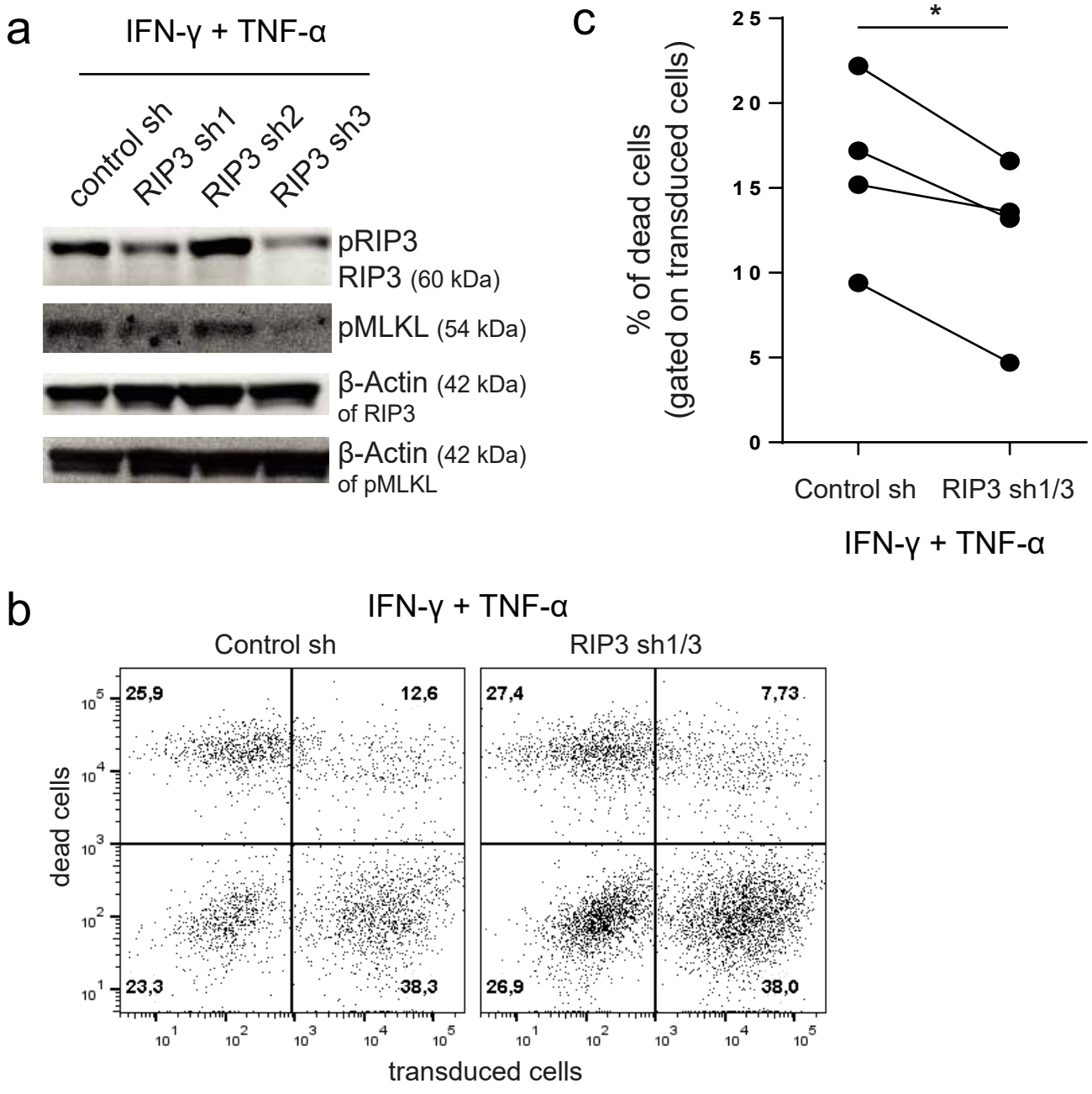
a
IFN-γ + TNF-α
control sh
RIP3 sh1
RIP3 sh2
RIP3 sh3
pRIP3
RIP3 (60 kDa)
pMLKL (54 kDa)
β-Actin (42 kDa)
of RIP3
β-Actin (42 kDa)
of pMLKL
c
*
% of dead cells
(gated on transduced cells)
25
20
15
10
5
0
Control sh
RIP3 sh1/3
IFN-γ + TNF-α
b
IFN-γ + TNF-α
Control sh
RIP3 sh1/3
dead cells
25,9
12,6
23,3
38,3
27,4
7,73
26,9
38,0
transduced cells

Supplemental Material

Type I immune response induces keratinocyte necroptosis and is associated with interface dermatitis

Felix Lauffer[1], Manja Jargosch[1], Linda Krause[2], Natalie Garzorz-Stark[1], Regina Franz[1], Sophie Roenneberg[1], Alexander Böhner[1], Nikola S. Mueller[2], Fabian J. Theis[2,4], Carsten B. Schmidt-Weber[3], Tilo Biedermann[1], Stefanie Eyerich[3], Kilian Eyerich[1]

Affiliations:

[1] Department of Dermatology and Allergy, Technical University of Munich, Munich, Germany

[2] Institute of Computational Biology, Helmholtz Center Munich, Neuherberg, Germany

[3] ZAUM – Center of Allergy and Environment, Technical University and Helmholtz Center Munich, Munich, Germany

[4] Department of Mathematics, Technical University of Munich, Garching, Germany

Table of content

Supplementary material and methods

Pre-processing of microarray data

Gene expression microarrays of human skin biopsies and keratinocytes were pre-processed together and analysed in parallel. The *limma* package was used to load the arrays into R (Ritchie et al., 2015, Team, 2016). The quality of the arrays was assessed using the *arrayQualityMetrics* package (Kauffmann et al., 2009). Background correction (*normexp* method) and quantile normalization between different arrays was performed using the *limma* package. For mapping of probe identifiers to gene symbols the annotation provided by Agilent was used.

Modelling the gene expression data

Two model set-ups were used to analyse the gene expression data. First, gene expression of LP, LE and psoriasis skin biopsies was analysed regarding all three diseases as separate predictor variables in comparison to the autologous healthy measurement. Second, we combined both interface diseases in one predictor and compared it to autologous healthy skin and psoriasis gene expression. To adjust for inter-individual variability, we fitted in both models a linear mixed-effects model using the restricted maximum likelihood criterion where individual patients were included as random effects in the model (=random intercepts). We calculated one model per probe measurement and set-up. Estimated coefficients of these models are equivalent to and shall be referred to as “fold changes” within this manuscript. Corresponding p values were calculated using the *Kenward-Roger* approximation for the denominator degrees of freedom and adjusted for multiple testing. To reveal differences and similarities between keratinocyte and ID gene expression we performed a correlation analysis between the fold changes of the genes of interest using Pearson's product-moment correlation. P values were adjusted for multiple testing using *Benjamini Hochberg* correction (Singmann H, 2015). Genes are regarded as significant if the adjusted p value is below 0.05. Top genes were defined based on the level of the absolute fold change.

Cell culture

HEK 293LTV cells (Cellbiolabs) were cultured in Dulbecco's modified Eagle's medium supplemented with 10 % fetal calf serum (FCS), 0.1 mM non-essential amino acids (NEAA), 2 mM L-Glutamine and 100 U/ml penicillin/streptomycin at 37 °C, 5 % CO_2.

Primary human epidermal keratinocytes were obtained by suction blister and cultured in DermaLife Basal Medium supplemented with DermaLife K LifeFactor Kit (Lifeline Cell Technology) at 37 °C, 5 % CO_2. Second- to third-passage primary human epidermal keratinocytes were used and cultured in 6-well plates with a starting cell number of 0.2 x 10^6. For stimulation, cells were starved for 5 hours in DermaLife Basal Medium without supplements following stimulation with human recombinant IFN-γ/TNF-α (R&D systems), human recombinant IFN-α A/D (R&D systems) or mixed T cell supernatant obtained from lesional T cells of LP and LE biopsies for 16 hours (western blot analysis) or 72 hours (three-dimensional skin model) in supplemented DermaLife Basal Medium without hydrocortisone.

Lentiviral vector construction

The lentiviral vector for shRNA knockdown pLL3.7 was a gift from Luk Parijs (Addgene plasmid #11795) (Rubinson et al., 2003). Non-targeting control and RIP3 (NM_006871) shRNA sequences (mRNA target sequences: control sh = GTTATTCGCGCGAATAACG; RIP3 sh1 = GCCACAGGGTTGGTA TAAT; RIP3 sh2 = GGAGAACAATATGAATGCT; RIP3 sh3 = GGGTTATCGAGAAGGT GAA) were synthezised by metabion with 5' *HpaI* and 3' *XhoI* overhangs. After hybridisation of sense and anti-sense strand and 5' phosphorylation by T4 poly nucleotide kinase, shRNA sequences were cloned into pLL3.7 at *HpaI* and *XhoI* restriction sites.

Lentiviral vector production

Virus supernatant was obtained by transfection of the following plasmids into HEK 293LTV cells using Turbofect (Thermo Scientific) as transfection reagent according to the manufacturer's instructions: two packaging plasmids (pRSV-REV [1.875 µg] and pCgpV [3.750 µg]), an envelope plasmid (pCMV-VSV-G [1.875 µg]) and the transfer plasmid (pLL3.7 [7.5 µg]). One day after transfection the serum was reduced to 2 % FCS in the medium. Pseudoviral particles were collected two and three days after

transfection. Using Amicon Ultra-15 Centrifugal Filter Devices 100K (Merck Millipore) the lentiviral supernatant was concentrated and filtered through 0.45 µm pore-size filter. To determine the transfection efficiency, the percentage of GFP-positive cells was further analysed by flow cytometry.

Lentiviral Transduction of primary human epidermal keratinocytes

Second-passage primary human epidermal keratinocytes were cultured in six-well plates and transduced with freshly concentrated lentiviral supernatant on two consecutive days. Here, prior to infection culture medium was removed, and the cells were infected with 2 mL of concentrated lentiviral supernatant in the presence of 8 µg/ml polybrene by centrifugation (800 xg) for 90 minutes at 32°C and rested for further 3.5 hours at 37°C before removal of the lentiviral supernatant and addition of full keratinocyte medium. Three days after the second transduction the cells were harvested and used for western blot analysis or for the three-dimensional skin model. To determine the transfection efficiency, the percentage of GFP-positive cells was further analysed by flow cytometry.

Isolation of lesional T cells

Primary human T cells were isolated from freshly taken skin biopsies and cultured in Roswell Park Memorial Institute (RPMI) 1640 medium supplemented with 5 % human serum, 0.1 mM NEAA, 2 mM L-Glutamine, 1 mM sodium pyruvate and 100 U/ml penicillin/streptomycin at 37 °C, 5 % CO_2. Skin biopsies were placed in 24-well plates with medium containing 60 U/ml IL-2. Fresh medium containing 60 U/ml IL-2 was replaced three times a week. Lesional T cells emigrated from tissue samples were expanded by α-CD3 and α-CD28 stimulation (each 0.75 µg/ml, α-CD3 pre-coated in PBS, α-CD28 soluble) and harvested for flow cytometry analysis.

Three-dimensional skin models

0.25 x 10^6 primary human keratinocytes were seeded on a polycarbonate membrane with 0.4 µm diameter pore size in keratinocyte medium containing 1.5 mM $CaCl_2$ and cultured at 37 °C in a humidified atmosphere containing 5 % CO_2. After 24 hours keratinocytes were exposed to the air-liquid interface and the surrounding medium was replaced with fresh keratinocyte medium containing 1.5 mM $CaCl_2$ and 50 µg/ml vitamin. The medium was changed every two days and keratinocytes were cultured

for another 10-13 days. Skin models were stimulated by adding stimuli to the surrounding medium for 72 hours. Skin models were fixed in 4 % formalin, embedded in paraffin and 5 µm sections were stained with haematoxylin and eosin.

Western blot analysis

Keratinocytes were lysed in RIPA lysis buffer (Santa Cruz) supplemented with 2 mM PMSF, proteinase inhibitor cocktail (1:70) and 1 mM sodium orthovanadate according to the manufacturer's instructions. Equal protein concentrations – determined by BCA protein assay – were resolved by SDS-PAGE using Bolt 4-12 % Bis-TrisPlus Gels and analysed by western blot using enhanced chemiluminescence. For staining the following antibodies were used: rbαRIP3 (Abcam, 1:2000), rbαMLKL-P-S358 (Abcam, 1:1000), rbαCleaved Caspase-3 (Cell Signaling, 1:1000), mαbAct (Sigma, 1:10000), αrbHRP (SantaCruz, 1:10000) and αrbHRP (Jackson, 1:10000).

Quantification of immunohistochemical staining

T-bet positive cells and cleaved caspase 3 positive cells were counted in two visual fields (400x) per condition by two independent investigators in a blinded manner and mean was calculated. Mean diaminobenzidine (DAB) intensity was measured using ImageJ software and colour deconvolution plugin as described before (Ruifrok and Johnston, 2001, Schindelin et al., 2012, Schindelin et al., 2015). Briefly, high resolution images (100x) were obtained under standadized light conditions. Mean DAB intensity was measure after inverting the image in an epidermal area of 100 x 300µm (0.03 mm^2). Size of the area was determined by the thickness of the smallest epidermis of the samples measured.

References

Kauffmann A, Gentleman R, Huber W. arrayQualityMetrics--a bioconductor package for quality assessment of microarray data. Bioinformatics 2009;25(3):415-6.

Ritchie ME, Phipson B, Wu D, Hu Y, Law CW, Shi W, et al. limma powers differential expression analyses for RNA-sequencing and microarray studies. Nucleic acids research 2015;43(7):e47.

Rubinson DA, Dillon CP, Kwiatkowski AV, Sievers C, Yang L, Kopinja J, et al. A lentivirus-based system to functionally silence genes in primary mammalian cells, stem cells and transgenic mice by RNA interference. Nature genetics 2003;33(3):401-6.

Ruifrok AC, Johnston DA. Quantification of histochemical staining by color deconvolution. Analytical and quantitative cytology and histology 2001;23(4):291-9.

Schindelin J, Arganda-Carreras I, Frise E, Kaynig V, Longair M, Pietzsch T, et al. Fiji: an open-source platform for biological-image analysis. Nature methods 2012;9(7):676-82.

Schindelin J, Rueden CT, Hiner MC, Eliceiri KW. The ImageJ ecosystem: An open platform for biomedical image analysis. Molecular reproduction and development 2015;82(7-8):518-29.

Singmann H BB, Westfall J, Aust F. afex: Analysis of Factorial Experiments. R package version 0.15-2. . 2015.

Team RC. R: A language and environment for statistical computing. R Foundation for Statistical Computing, Vienna, Austria 2016.

Supplementary Table S1 Top 500 genes differentially regulated in lichen planus and lupus erythematosus

Agilent SurePrint G3 GE 8x60k ID	HGNC Symbol	fold change	adj. p-value
A_23_P18452	CXCL9	5.68917721	5.69928E-11
A_24_P303091	CXCL10	5.498943281	4.23596E-11
A_33_P3343175	CXCL10	5.456078997	3.62616E-11
A_23_P125278	CXCL11	4.847845117	1.35509E-10
A_33_P3289845	IGFL1	4.513854415	9.43922E-10
A_23_P38537		4.446273829	4.2797E-10
A_23_P23048		4.430866718	3.28314E-08
A_23_P1691	MMP1	4.366216056	1.32504E-07
A_33_P3391895	HRNR	4.289678735	1.93212E-06
A_23_P74290	GBP5	4.26509697	1.95115E-12
A_23_P139786	OASL	4.073152012	4.88666E-12
A_23_P117602	GZMB	4.07307306	5.30547E-12
A_33_P3405424	IL4I1	3.982204484	5.54458E-12
A_23_P121695	CXCL13	3.963755416	3.18596E-13
A_24_P117410	KLHDC7B	3.955472505	1.77566E-12
A_23_P434809	S100A8	3.942850763	2.46921E-08
A_23_P210465	PI3	3.91245544	2.73361E-08
A_23_P6535	KLHDC7B	3.878373263	9.0958E-12
A_23_P152838	CCL5	3.871854176	5.25981E-12
A_23_P366936		3.777891113	2.68642E-07
A_23_P156218	GZMK	3.750909445	3.62616E-11
A_23_P209954	GNLY	3.745600841	1.42362E-11
A_23_P343398	CCR7	3.726756277	4.88666E-12
A_23_P97141	RGS1	3.703965281	3.81673E-13
A_33_P3375859	CXCR2P1	3.683940143	2.36221E-10
A_33_P3316273	CCL3	3.683786804	1.44247E-11
A_23_P114299	CXCR3	3.608820191	3.13971E-13
A_32_P44394	AIM2	3.608412958	4.55622E-12
A_33_P3396139	CTLA4	3.598121934	6.56524E-14
A_23_P81898	UBD	3.589311327	8.94664E-12
A_23_P81898	GABBR1	3.589311327	8.94664E-12
A_23_P357717		3.539552625	7.54163E-10
A_23_P63390	FCGR1CP	3.538629828	5.7064E-11
A_23_P63390	FCGR1A	3.538629828	5.7064E-11
A_23_P63390	FCGR1B	3.538629828	5.7064E-11
A_23_P404494	IL7R	3.538321541	1.80996E-11
A_33_P3376821	GZMA	3.494107118	1.40229E-11
A_23_P103310		3.469485481	2.23571E-05
A_23_P151046	KLRC1	3.446950723	3.237E-12
A_23_P161076	CD2	3.436089667	1.95115E-12
A_33_P3400273	SELL	3.426177979	5.60949E-10
A_23_P371215	ICOS	3.35863675	6.56524E-14

A_23_P55632	SERPINB3	3.351728881	1.39515E-08
A_23_P119042	NKG7	3.338654138	2.13933E-10
A_23_P112026	IDO1	3.318964907	4.01808E-11
A_32_P163247	CD8A	3.300598534	9.22921E-12
A_23_P92909	SPINK6	3.278638528	1.14985E-05
A_23_P98410	CD3G	3.276819295	7.35447E-12
A_23_P40174	MMP9	3.26630576	7.4468E-12
A_23_P7827	FAM26F	3.259843679	1.02078E-11
A_24_P183128		3.252293191	1.17472E-09
A_33_P3292886	KRT6A	3.249011222	5.38051E-08
A_33_P3351745	PVRIG	3.241969952	2.73021E-12
A_33_P3351745	STAG3	3.241969952	2.73021E-12
A_24_P28722	RSAD2	3.231781288	1.25382E-07
A_23_P116942		3.226887799	8.0393E-12
A_33_P3354607	CCL4	3.210382165	8.28588E-12
A_23_P502413	SERPINB4	3.204845656	5.33031E-08
A_23_P207564	CCL4	3.198224482	3.16345E-12
A_23_P311875	CD6	3.197800422	2.41273E-12
A_33_P3328559	TBC1D10C	3.171978832	3.4493E-12
A_33_P3260654	TRBC2	3.161547857	4.88666E-12
A_23_P370682	BATF2	3.156416998	9.41156E-11
A_33_P3375541	CD3D	3.154462197	3.62616E-11
A_23_P157628	DEFB4B	3.151563141	1.11563E-05
A_23_P157628	DEFB4A	3.151563141	1.11563E-05
A_23_P34676	CD247	3.13941757	2.73021E-12
A_33_P3248265	LTB	3.133285879	2.24637E-11
A_23_P201459	IFI6	3.104372818	4.87142E-09
A_23_P28857	SIRPG	3.102175208	1.32264E-13
A_23_P93641	AKR1B10	3.091588944	3.21697E-09
A_24_P340128	P2RY8	3.080383192	5.45349E-12
A_33_P3342056	TIGIT	3.078526306	1.37375E-12
A_19_P00812504		3.066412386	1.37375E-12
A_33_P3283619	SH2D1A	3.055390023	5.45349E-12
A_19_P00800763		3.054713933	3.62616E-11
A_24_P45476	XCL2	3.054517501	3.62616E-11
A_24_P45476	XCL1	3.054517501	3.62616E-11
A_33_P3368334	FCRL3	3.053329664	5.45349E-12
A_19_P00322900	MIAT	3.049654067	6.50413E-12
A_24_P97374	EOMES	3.044735136	3.76071E-11
A_33_P3424577		3.039349182	4.88666E-12
A_19_P00321068	MIAT	3.037606761	1.08638E-11
A_23_P819	ISG15	3.03378758	1.88043E-08
A_23_P206806	ITGAL	3.02203489	6.6171E-13
A_23_P323761	TRAF3IP3	3.019038473	3.237E-12
A_23_P105794		3.009913221	5.33775E-11
A_23_P340019	NLRC3	3.005514464	7.4468E-12
A_23_P306941	RGL4	3.005398844	5.30547E-12

A_24_P59667	JAK3	3.000180596	1.77566E-12
A_33_P3214948	SPOCK2	2.995139375	8.78573E-12
A_19_P00315524	MIAT	2.970414047	4.56724E-11
A_19_P00317953		2.966041229	2.2659E-11
A_33_P3283611	IFIT3	2.925091818	2.91213E-08
A_24_P129341	AKR1B10P1	2.924469744	6.21804E-10
A_24_P129341	AKR1B10	2.924469744	6.21804E-10
A_33_P3364821	PTPRC	2.921482595	3.96338E-12
A_24_P205994	EPGN	2.916562699	3.7428E-08
A_24_P274270	STAT1	2.912044823	3.96338E-12
A_23_P23074	IFI44	2.910977812	7.04564E-10
A_23_P102000	CXCR4	2.907650927	7.63308E-11
A_23_P32404	ISG20	2.904963827	1.98859E-10
A_19_P00321067	MIAT	2.900865535	1.39986E-11
A_24_P237443		2.899014246	1.67562E-12
A_24_P237443	SASH3	2.899014246	1.67562E-12
A_23_P253317	GPR171	2.896878992	3.96338E-12
A_23_P76249	KRT6B	2.889119443	1.44761E-07
A_33_P3387691	SCML4	2.87342149	2.49163E-08
A_23_P109913	CXCR6	2.857804098	3.44214E-12
A_33_P3343120	IRF8	2.856730932	4.0399E-11
A_24_P353638	SLAMF7	2.856365281	2.73021E-12
A_23_P17663	MX1	2.841574949	2.85163E-09
A_33_P3380992	AKR1B10	2.828492769	1.74441E-09
A_33_P3380992	AKR1B15	2.828492769	1.74441E-09
A_23_P218058	KLRC4	2.823329443	6.85791E-12
A_23_P218058	KLRC4-KLRK1	2.823329443	6.85791E-12
A_19_P00322332		2.819785389	4.08982E-11
A_19_P00806066		2.818843238	6.69574E-11
A_23_P412321	CCR5	2.810840924	8.28588E-12
A_33_P3382746	LCK	2.808247321	4.86349E-12
A_33_P3421351	TRAF3IP3	2.807082235	1.82663E-11
A_23_P153372	HSH2D	2.805954756	5.08507E-11
A_23_P103361	LCK	2.800122688	6.6171E-13
A_24_P854492	MIAT	2.794198214	1.4936E-11
A_23_P58132	RHOH	2.793675207	6.48119E-13
A_33_P3298990	CD5	2.784471725	5.48362E-11
A_33_P3462422	THEMIS	2.773718492	1.17109E-10
A_23_P74547	CD53	2.769908469	2.31787E-12
A_33_P3364811	PTPRC	2.761245149	3.08387E-11
A_33_P3208970	ZNF683	2.759917192	1.93135E-10
A_23_P12392	PTPRC	2.757374347	3.01081E-10
A_23_P48088	CD27	2.757127785	3.69411E-12
A_23_P48088	TAPBPL	2.757127785	3.69411E-12
A_23_P128993	GZMH	2.73971919	2.08332E-09
A_23_P93524		2.737491872	1.67766E-09
A_23_P93524	SAMD3	2.737491872	1.67766E-09

A_32_P206479	ZNF831	2.737484979	1.08638E-11
A_32_P101352	CXorf65	2.730268667	1.93135E-10
A_23_P62890	GBP1	2.728910949	8.80834E-09
A_33_P3281273	S1PR4	2.724440572	4.88849E-11
A_32_P56249	USP30-AS1	2.723488372	2.30669E-11
A_24_P280274	S100A7A	2.713781373	2.18616E-05
A_32_P175934	CD48	2.707382689	5.7447E-10
A_23_P115519	LCE3D	2.706790609	8.06021E-08
A_23_P55270	CCL18	2.705936233	0.001256371
A_23_P127288	IL2RA	2.703944112	4.56724E-11
A_33_P3401826	CMPK2	2.700622513	5.458E-08
A_24_P227927	IL21R	2.697904466	1.74004E-12
A_23_P45871	IFI44L	2.692856387	1.95808E-06
A_23_P79069	RASAL3	2.675520779	5.39716E-11
A_24_P941167	APOL6	2.652071473	6.51716E-10
A_33_P3220911	BST2	2.647696619	2.94125E-09
A_33_P3267799	LILRB4	2.639028658	1.71644E-10
A_23_P204087	OAS2	2.634143337	1.04416E-09
A_33_P3295056	CORO1B	2.624452648	1.8296E-11
A_33_P3295056	PTPRCAP	2.624452648	1.8296E-11
A_33_P3247431	SPRR2B	2.616946308	0.000567288
A_24_P161018	PARP14	2.616567225	5.59042E-11
A_23_P201778	PTPN7	2.610882079	2.41273E-12
A_33_P3268555	SP140	2.602728473	2.73021E-12
A_23_P212568	TRAT1	2.600730962	6.47091E-11
A_33_P3264179	LCE3E	2.598787681	1.56433E-07
A_23_P87879	CD69	2.590479916	4.47022E-09
A_23_P90626	CYTIP	2.578835643	3.14011E-11
A_23_P44155	CD96	2.577606759	3.62616E-11
A_33_P3380383	TIFAB	2.574291908	3.48916E-11
A_23_P39465	BST2	2.572005876	1.26757E-08
A_23_P141555	TBX21	2.570074584	9.53202E-12
A_19_P00804124	TRAC	2.544792159	1.13997E-11
A_23_P207456	CCL8	2.541722316	2.46966E-07
A_33_P3281403	TRAF3IP3	2.538915505	9.88741E-12
A_24_P328504		2.537155039	2.73021E-12
A_23_P131024	ZBTB32	2.520295688	3.237E-12
A_24_P393740	FYB	2.516692137	6.47985E-11
A_23_P28334	IL18RAP	2.513994264	3.07299E-10
A_24_P169234		2.512748003	8.05169E-12
A_24_P557479	XAF1	2.495624215	3.00155E-10
A_32_P232559	PRKCQ-AS1	2.495245591	3.48916E-11
A_23_P91095	CD28	2.472224388	3.62616E-11
A_23_P145874	SAMD9L	2.470004652	8.04408E-11
A_23_P167328	CD38	2.463915495	7.80406E-07
A_23_P166797	RTP4	2.459769453	6.51992E-10
A_23_P354151	ITK	2.457192186	3.29783E-11

A_23_P68155	IFIH1	2.446443852	7.7729E-10
A_23_P21057		2.441962875	1.0242E-11
A_23_P21057	SEPT1	2.441962875	1.0242E-11
A_33_P3406196	KLRD1	2.439764347	7.18301E-09
A_33_P3259393	HAPLN3	2.437564898	5.25981E-12
A_23_P346093	TMC8	2.430856102	1.56203E-11
A_23_P123853	CCL19	2.424104619	1.02998E-07
A_24_P378019	IRF7	2.419713901	4.56724E-11
A_33_P3390172	ADAMDEC1	2.417765578	3.62616E-11
A_23_P143713	APOBEC3G	2.409704025	1.76948E-09
A_23_P120902	LGALS2	2.408586959	7.86652E-09
A_23_P41765	IRF1	2.404736815	8.29609E-12
A_23_P259141	ZBP1	2.392924751	5.99975E-10
A_33_P3842556	IKZF1	2.392910539	1.34789E-10
A_33_P3235213	TIGIT	2.387199027	2.31787E-12
A_32_P216520	WIF1	-2.387104845	7.80107E-08
A_23_P369471	LCE3A	2.383330113	2.37752E-07
A_33_P3309526	PTPRC	2.379421818	9.75688E-12
A_33_P3297345	TTC24	2.378012415	1.98708E-09
A_23_P70670	CD83	2.374580906	1.08638E-11
A_33_P3246838	TRDC	2.374501986	7.31483E-08
A_23_P204208	KLRD1	2.372998143	4.84045E-09
A_33_P3225625	TRGC2	2.364245128	2.16848E-11
A_33_P3225625	TRGC1	2.364245128	2.16848E-11
A_33_P3258346	XAF1	2.354751995	4.49133E-09
A_19_P00812190		2.3519462	5.57528E-09
A_23_P29005	SAMSN1	2.349097622	1.39941E-10
A_33_P3224710	TFEC	2.345021973	1.87936E-09
A_33_P3241021	CD69	2.339201851	1.4555E-09
A_24_P335305	OAS3	2.333536838	2.08098E-09
A_33_P3341616	GVINP1	2.333460946	1.63167E-11
A_33_P3353816		2.328935809	4.08982E-11
A_23_P128974	BATF	2.327666993	2.41139E-10
A_23_P398566	NR4A3	2.324455864	2.84685E-10
A_23_P6263	MX2	2.322465523	2.40934E-08
A_23_P6293	UBASH3A	2.319733394	9.37374E-12
A_23_P43369	SIT1	2.312184281	8.05169E-12
A_33_P3253687	GVINP1	2.308175905	3.00155E-10
A_23_P15146	IL32	2.30262761	6.32221E-10
A_23_P15146	RNU1-125P	2.30262761	6.32221E-10
A_24_P251950	UGT3A2	-2.291021151	4.93094E-09
A_23_P98350	BIRC3	2.289711883	4.81331E-09
A_23_P29773	LAMP3	2.288119691	1.72594E-10
A_23_P84596	MZB1	2.28063352	9.27842E-08
A_23_P64661	ARHGAP9	2.279838416	3.62616E-11
A_33_P3231414	LILRB1	2.275229591	7.35328E-08
A_23_P14174	TNFSF13B	2.274664003	5.68675E-11

A_23_P31725	BLK	2.274214928	8.67498E-10
A_23_P200138	SLAMF8	2.269123938	4.69947E-10
A_24_P45446	GBP4	2.268966471	2.21842E-08
A_33_P3290394	IL2RG	2.266100548	1.64108E-11
A_23_P1374	PRKCQ	2.26466522	1.40229E-11
A_24_P944253	KLHL6	2.262321243	3.57538E-11
A_23_P39067	SPIB	2.255712731	8.67498E-10
A_23_P97112	SELE	2.241995269	5.57624E-08
A_23_P200728	FCGR3A	2.238371414	2.31755E-07
A_23_P81441	DCANP1	2.231766414	2.56757E-10
A_23_P81441	TIFAB	2.231766414	2.56757E-10
A_33_P3352827	SLAMF1	2.231055638	1.03445E-10
A_23_P86653	SRGN	2.230337631	4.54395E-09
A_23_P315364	CXCL2	2.229150403	4.99452E-08
A_23_P369815	FASLG	2.224903368	9.14787E-10
A_33_P3237674	TRAC	2.215587698	8.12012E-09
A_23_P211561	MEI1	2.215111055	2.6163E-10
A_24_P270460	IFI27	2.213352217	8.30987E-09
A_32_P190951	IGHV1-46	2.208482412	2.6006E-08
A_23_P64828	OAS1	2.207992975	8.44062E-08
A_23_P23639	MCOLN2	2.205102882	1.15329E-10
A_33_P3333960	LINC00426	2.204679503	7.86178E-11
A_23_P137366	C1QB	2.202742706	4.40276E-10
A_23_P56505	ITGA4	2.200546744	1.11152E-09
A_32_P30905	WDFY4	2.198438955	3.72804E-11
A_23_P64898	KLRG1	2.19732313	1.18322E-09
A_33_P3264846	SAMD9L	2.19562956	1.10762E-08
A_33_P3401556	CTLA4	2.194626367	6.66111E-12
A_24_P355626	ABCG4	2.186553164	1.16403E-09
A_23_P85800	CD52	2.182214983	2.91213E-08
A_33_P3227443	C16orf54	2.176068629	4.28213E-09
A_33_P3227443	C16orf54	2.176068629	4.28213E-09
A_23_P128281		2.17582954	5.18881E-09
A_33_P3357609	ZBP1	2.16743842	4.10082E-07
A_24_P192914	JAML	2.167364216	5.29038E-11
A_33_P3209651	WDFY4	2.164709808	1.73856E-09
A_23_P159406	SPRR1B	2.164262621	1.37819E-07
A_33_P3241984	PTPN22	2.162547095	7.35447E-12
A_33_P3283616	SH2D1A	2.157185828	3.96338E-12
A_23_P12082		2.152475239	4.02484E-06
A_23_P52266	IFIT1	2.151789366	2.50391E-05
A_23_P152002	BCL2A1	2.151334251	3.19406E-09
A_33_P3339376	WIPF1	2.143899184	1.82584E-08
A_33_P3377151	CCL19	2.137296611	5.26348E-07
A_24_P300777	ADAM8	2.137127693	6.69574E-11
A_33_P3315779	HERC6	2.133688879	5.0387E-05
A_33_P3318414	ARHGAP45	2.132433109	3.95655E-11

A_23_P433229	PHYHIP	-2.127926702	4.00849E-08
A_24_P11061		2.123954733	2.2368E-06
A_24_P230563	IL2RA	2.122020813	2.56536E-06
A_32_P9543	APOBEC3A	2.121659713	0.001552063
A_32_P9543	APOBEC3A	2.121659713	0.001552063
A_23_P100730	SKAP1	2.120543932	2.86444E-10
A_23_P30547	LCP2	2.117164397	9.56823E-11
A_33_P3225512	OAS2	2.116842669	2.5927E-08
A_33_P3406567	MS4A1	2.116554398	3.09016E-09
A_33_P3303857	SLAMF6	2.116085215	9.30936E-10
A_23_P314250	FAM78A	2.113287277	1.71644E-10
A_33_P3414880		2.102686044	2.77696E-09
A_33_P3316544	PARP15	2.095066275	2.08332E-09
A_23_P312132	ITGAX	2.094461941	5.54842E-11
A_23_P208493	LILRB2	2.093454142	3.1305E-07
A_23_P78092		2.091383901	1.81989E-10
A_23_P78092	EVI2A	2.091383901	1.81989E-10
A_24_P354724	TAGAP	2.090586043	5.68675E-11
A_23_P305198	STAT4	2.087515102	1.02547E-09
A_23_P203173	IL10RA	2.085144926	2.2659E-11
A_33_P3398251	FOXP3	2.084173143	5.01183E-12
A_33_P3229918	PTCRA	2.080183718	4.47138E-07
A_23_P14564	GPR65	2.077278863	2.14557E-09
A_24_P295010	SERPINB9	2.075959061	2.41139E-10
A_23_P24384	CCDC88B	2.075736291	1.51545E-10
A_33_P3286157	TNFRSF4	2.071800758	3.21388E-10
A_23_P40295	LAMP5	2.066044541	3.22349E-08
A_23_P25566	GPR183	2.059115677	1.60733E-09
A_24_P203103	SH2D1A	2.058663517	1.18322E-09
A_24_P98109	SNX10	2.050058083	4.90839E-10
A_32_P209960	CIITA	2.048091547	9.05385E-11
A_23_P27606	IL27RA	2.046696002	1.93135E-10
A_23_P14165	GPR18	2.043290553	1.13491E-10
A_23_P62647	SLAMF1	2.043246676	4.56724E-11
A_24_P148717	CCR1	2.041659587	1.1359E-07
A_23_P74012	SPRR1A	2.037947938	4.60202E-05
A_24_P12690	IDO2	2.033036204	1.46884E-08
A_24_P139604	PYHIN1	2.032897482	3.14011E-11
A_23_P73429		2.03021291	4.88666E-12
A_23_P68601		2.029488739	1.70935E-09
A_23_P136405	PDCD1	2.028905121	5.33813E-11
A_23_P376060	IKZF3	2.022255042	3.07299E-10
A_19_P00317052	RNF213	2.021777333	4.74414E-10
A_23_P99275	KLRB1	2.01959027	7.0201E-08
A_23_P48997	PSTPIP1	2.01908574	4.86349E-12
A_33_P3346826	IL32	2.016277302	1.02915E-09
A_19_P00322333		2.014845436	2.83347E-10

A_24_P237036	TNFSF14	2.008296522	1.66594E-09
A_24_P172481	TRIM22	2.006984177	1.11159E-07
A_24_P175187	SAMD9	2.005251453	6.87647E-08
A_23_P209678	PLEK	2.00153527	7.41235E-08
A_19_P00320293		1.998940387	2.24298E-09
A_23_P64058	RASGRP2	1.997582302	8.16811E-09
A_23_P84154		1.99517485	1.59246E-08
A_33_P3381255	CLEC2A	-1.992242468	3.3773E-06
A_23_P107336	ACAP1	1.991696952	4.50864E-11
A_23_P125977	C1QC	1.991332414	2.61462E-10
A_24_P304071	IFIT2	1.982929629	3.43451E-05
A_24_P13831	SNX20	1.978566653	4.86349E-12
A_23_P11070	GPR174	1.978358729	5.01091E-10
A_23_P7144	CXCL1	1.974501765	0.000551401
A_23_P250358	HERC6	1.972617971	1.68159E-06
A_23_P360754	ADAMTS4	1.971984046	1.58218E-07
A_23_P153745		1.970313131	3.68572E-09
A_32_P70158	LILRB3	1.969645712	3.9002E-07
A_32_P70158	LILRB3	1.969645712	3.9002E-07
A_32_P70158	LILRB3	1.969645712	3.9002E-07
A_32_P70158	LILRB3	1.969645712	3.9002E-07
A_23_P338479	CD274	1.969343419	4.27413E-08
A_24_P82749	CD37	1.96668528	3.91123E-10
A_23_P155057	CYTH4	1.964247464	1.88177E-09
A_33_P3235940	KLK6	1.96356981	0.002716917
A_32_P452655	LGALS9	1.959301886	5.49896E-10
A_32_P452655	LGALS9B	1.959301886	5.49896E-10
A_32_P452655	LGALS9C	1.959301886	5.49896E-10
A_32_P452655	LGALS9DP	1.959301886	5.49896E-10
A_23_P63032		-1.959298378	2.37965E-07
A_24_P307964	SOHLH1	-1.954803764	0.000182271
A_24_P379104		1.948079559	1.77566E-12
A_33_P3260614	PLCB2	1.945369496	3.63564E-10
A_33_P3350094	PATL2	1.941845721	1.40058E-08
A_32_P145010		1.939113578	2.73021E-12
A_23_P305092	CRTAM	1.938948234	1.242E-09
A_33_P3392405	C10orf99	1.936829536	0.000514982
A_23_P312920	POU2AF1	1.936581528	5.71564E-07
A_24_P365767	CYBB	1.932463023	2.49163E-08
A_23_P39386	HCST	1.931286408	1.274E-08
A_23_P258088	PACSIN1	1.930540637	1.66211E-07
A_23_P145718		1.925635424	1.5847E-08
A_23_P212655	KLHL6	1.924477289	3.62616E-11
A_23_P5002	MAP4K1	1.920615359	4.56724E-11
A_24_P272515	FABP5P10	1.913643187	5.96441E-07
A_24_P142305	HBA2	-1.908929	0.005171523
A_24_P142305	HBA1	-1.908929	0.005171523

A_23_P23783	MYOC	-1.897395456	2.55861E-06
A_23_P66694	EVI2B	1.891499992	1.62774E-09
A_23_P374082	ADAM19	1.891290606	1.32425E-10
A_33_P3225522	OAS2	1.891213199	1.2675E-07
A_33_P3237927	ARHGAP4	1.88890955	1.41011E-10
A_23_P140190	FAM30A	1.887466458	7.74074E-09
A_33_P3263319	IGHG3	1.884789344	0.023679456
A_23_P142424	IGFLR1	1.882800876	5.40845E-11
A_23_P142424		1.882800876	5.40845E-11
A_24_P567298		1.881432569	3.35171E-06
A_24_P206343		1.879588481	9.96012E-11
A_19_P00320834	TRAJ4	1.879411967	9.1314E-09
A_19_P00320834	TRAJ3	1.879411967	9.1314E-09
A_23_P74001	S100A12	1.878615629	0.000682152
A_23_P152398		-1.875958914	0.020282123
A_33_P3247042	FPR3	1.875205442	1.19025E-09
A_23_P69383	PARP9	1.873890443	1.58051E-07
A_23_P368681	GIMAP2	1.873386486	2.37117E-08
A_33_P3371999	TPPP	-1.869922232	3.49372E-06
A_23_P119478	EBI3	1.868542243	9.22921E-12
A_23_P64611	P2RY6	1.867721448	1.2493E-11
A_33_P3319987		1.860335425	7.62872E-10
A_23_P387471	MICB	1.858084637	5.31631E-09
A_23_P204947	GJB2	1.856105294	4.51376E-05
A_23_P78608	DENND1C	1.854354187	5.26327E-11
A_33_P3367860	CHRM1	-1.853949556	1.38001E-07
A_23_P62227	CXorf21	1.852712273	1.22607E-10
A_23_P158725	SLC16A3	1.850179099	5.42046E-08
A_23_P68436	WFDC12	1.849456264	0.000169798
A_23_P24004	IFIT2	1.847704653	0.000284206
A_24_P416131	COTL1	1.845357836	2.34662E-07
A_23_P156687		1.844345801	6.62902E-06
A_24_P153840	FGD3	1.838734081	1.92904E-11
A_24_P241183	CLEC2D	1.837482916	1.34272E-07
A_23_P162386		1.83738744	8.85667E-08
A_24_P161764	IGHV1-3	1.836635303	7.01728E-07
A_33_P3382498	SIGLEC14	1.836127213	4.26076E-07
A_33_P3226154	IGKC	1.835088094	0.008385989
A_23_P41470	DDX60	1.834571195	7.4412E-07
A_23_P68031	STAT4	1.833922322	4.97541E-09
A_23_P24389		1.831432214	4.39804E-11
A_24_P48898	APOL2	1.830356544	5.28301E-11
A_24_P101651	CSAG4	1.828993995	4.41116E-06
A_32_P101031	LYPD1	1.828957711	3.5174E-07
A_33_P3250680	CD40LG	1.826263035	9.32429E-08
A_23_P132388	SCO2	1.825223626	1.16403E-09
A_23_P132388		1.825223626	1.16403E-09

A_24_P673063	FABP5P3	1.823332973	3.83173E-07
A_33_P3402489	OAS3	1.822611976	2.92365E-08
A_32_P54553	USP41	1.822144182	5.59101E-05
A_32_P204676	FABP5P7	1.81809892	5.458E-08
A_32_P204676	FABP5	1.81809892	5.458E-08
A_23_P250413	PARVG	1.817490372	1.05892E-12
A_23_P208866	GMFG	1.817119421	3.76714E-09
A_33_P3236020	TIMD4	1.8165917	1.34185E-06
A_23_P142447	MYO1F	1.814957412	3.46625E-10
A_23_P137935		1.812416482	1.2322E-07
A_19_P00323850		1.802486423	4.01589E-07
A_23_P64860	SELPLG	1.801314522	2.4946E-10
A_23_P51936	TNFRSF9	1.79710747	1.0242E-11
A_23_P38959	VAV1	1.796021611	7.59335E-10
A_24_P229531		1.794563242	1.50856E-09
A_33_P3218960	CACNA1H	-1.793154231	0.000490936
A_23_P148473	IL2RG	1.79181135	6.42666E-10
A_23_P65651	WARS	1.791685099	1.04703E-08
A_33_P3415032	KCNA3	1.788459211	1.1159E-10
A_23_P151294	IFNG	1.787654821	6.696E-10
A_23_P139654	KLRC1	1.77853712	8.6422E-07
A_23_P106761	CORO1A	1.773530428	1.26773E-10
A_23_P149946	CDHR1	-1.770985647	3.09793E-07
A_23_P113572	CD19	1.770920776	4.13357E-08
A_33_P3385785	S100A12	1.768630996	0.001286488
A_23_P209129	LAIR2	1.767517988	9.7069E-08
A_33_P3372004	IGSF6	1.764725127	3.16684E-10
A_23_P23279	RCSD1	1.763770023	7.88953E-08
A_24_P362193	CD84	1.759393797	3.23387E-09
A_33_P3262635	CECR1	1.758226818	2.43578E-09
A_24_P295590	RASSF4	1.754671373	1.36636E-09
A_33_P3212172	SNX22	1.752623997	9.35056E-08
A_23_P132159	USP18	1.750323409	4.55091E-05
A_23_P132159		1.750323409	4.55091E-05
A_23_P30069		1.748872322	7.78642E-08
A_33_P3212232	MPEG1	1.748292976	2.3341E-08
A_33_P3369393	NCF1B	1.747782055	2.94948E-08
A_33_P3369393	NCF1	1.747782055	2.94948E-08
A_33_P3369393	NCF1C	1.747782055	2.94948E-08
A_24_P48204	SECTM1	1.746975292	1.61314E-06
A_33_P3398912	SLC2A6	1.745927535	3.07184E-08
A_24_P291658	ADH1A	-1.737500298	5.4916E-05
A_24_P291658	ADH1B	-1.737500298	5.4916E-05
A_23_P70095	CD74	1.736373911	6.00875E-08
A_23_P329573	ITGB2	1.729804566	7.13888E-09
A_23_P65629	KCNK10	1.728563516	2.86072E-07
A_33_P3227899		1.728498659	2.76387E-08

A_24_P246351	FAM71E1	-1.725850965	1.45709E-08
A_23_P209347	ANKRD44	1.725795818	2.18377E-09
A_24_P184799	COCH	-1.725243979	5.05036E-05
A_23_P34345	VCAM1	1.72496315	2.73361E-08
A_24_P193093	KLRK1	1.724222497	8.67498E-10
A_24_P193093	KLRK1	1.724222497	8.67498E-10
A_24_P193093	KLRC4-KLRK1	1.724222497	8.67498E-10
A_23_P111000	PSMB9	1.719014554	3.86863E-08
A_23_P259611	NME8	1.717052715	2.86403E-07
A_23_P85693		1.71702504	5.67181E-08
A_33_P3295348	CLEC2A	-1.716339956	4.38705E-05
A_24_P254833	TRBV7-9	1.712520137	2.7275E-10
A_33_P3352578	CLEC4D	1.711527148	1.00041E-06
A_24_P50950	CCDC88B	1.711030979	3.36293E-11
A_23_P90497		1.707890486	1.22786E-07
A_23_P90497	LILRA4	1.707890486	1.22786E-07
A_23_P348208	SPRR1A	1.706542811	1.76691E-06
A_23_P157879	FCN1	1.706436054	0.000300219
A_33_P3288359		1.705854152	4.48274E-11
A_33_P3288359	PSMB10	1.705854152	4.48274E-11
A_23_P7503	TIMD4	1.705193463	1.8171E-06
A_23_P36531	TSPAN8	-1.702074941	1.1282E-06
A_23_P161940		-1.701748749	0.039991695
A_24_P228149		-1.700022787	0.000162306
A_19_P00321017	TRAJ19	1.699283215	1.37371E-08
A_19_P00321017	TRAJ18	1.699283215	1.37371E-08
A_24_P367432		1.698007134	2.72685E-05
A_23_P204847	LCP1	1.696052382	1.5847E-08
A_23_P54770	APOBR	1.695235787	1.92035E-10
A_32_P351968	HLA-DMB	1.693551699	5.2548E-10
A_23_P212119	GALNT15	-1.69345538	0.000302523
A_23_P216340	SLA	1.693444309	1.11152E-09
A_33_P3421053	SELE	1.690618657	7.81236E-10
A_23_P218770	RAC2	1.689173205	1.98503E-08
A_23_P1962	RARRES3	1.689109334	7.7155E-09

Top 500 genes differentially regulated in lichen planus and lupus erythematosus compared to autologous healthy skin, sorted by absolute fold change.

Supplementary Table S2 Concentration of cytokines in the T cell supernatant mix

	not depleted	IFN-γ depleted	TNF-α depleted	IFN-γ and TNF-α depleted
TNF-α (pg/ml)	5713	7175	890	1126
IFN-γ (pg/ml)	8212	2787	7675	2229

Concentration of cytokines in the T cell supernatant mix before and after depletion.

Supplementary Table S3 Patient's characteristics

Patient #	Sex	Age	Diagnosis
1*	male	39	Lichen planus
2*	female	39	Lichen planus
3*	male	68	Lichen planus
4*	female	48	Lichen planus
5	female	71	Lichen planus
6*	male	62	Lichen planus
7	female	36	Lichen planus
8*	male	39	Chilblain lupus
9	female	71	Lupus erythematosus tumidus
10*	male	79	Subacute cutaneous lupus erythematosus
11*	male	63	Subacute cutaneous lupus erythematosus
12*	female	65	Discoid lupus erythematosus
13*	female	75	Lichen planus
14	female	53	Lichen planus
15*	female	47	Lichen planus
16*	female	61	Lichen planus
17*	male	40	Lichen planus
18*	female	56	Lichen planus
19	female	45	Subacute cutaneous lupus erythematosus
20*	female	14	Discoid lupus erythematosus
21	female	39	Discoid lupus erythematosus
22	female	54	Discoid lupus erythematosus
23*	female	54	Lichen planus
24	male	32	Lupus erythematosus tumidus
25	female	50	Subacute cutaneous lupus erythematosus
26	female	24	Psoriasis
27	male	17	Psoriasis
28	female	43	Psoriasis
29	female	55	Psoriasis
30	female	28	Psoriasis
31	female	53	Psoriasis
32	female	67	Psoriasis
33	female	35	Psoriasis
34	female	45	Psoriasis

* included in transcriptome analysis

Supplementary Table S4 Histological attributes

Histology criteria	Grading (e.g. 0=absent - 3=very strong)
suprapapillary epidermis	0-3
hyperkeratosis	0-3
parakeratosis (quantitative)	0-3
parakeratosis (qualitative)	0-3
orthokeratosis	0-3
acanthosis (quantitative)	0-3
acanthosis (qualitative)	0-3
granulosis	0-3
serum crust	yes/no
spongiosis	0-3
dilated intrapapillary capillaries	0-3
dermal lymphocytes	0-3
lymphocytic exocytosis	0-3
microabscess	yes/no
detection of bacteria	yes/no
neutrophils (quantitative)	0-3
neutrophils (qualitative)	0-3
eosinophils	0-3
interface dermatitis (quantitative)	0-3
suprabasal dyskeratotic cells	yes/no
number of dyskeratotic cells	absolute number
distribution of interface dermatitis	0-3
interface dermatitis (qualitative)	0-3
leucocytoclasia	0-3

Supplementary Figure S1 Regulation of genes belonging to “apoptosis” and “necroptosis” pathway

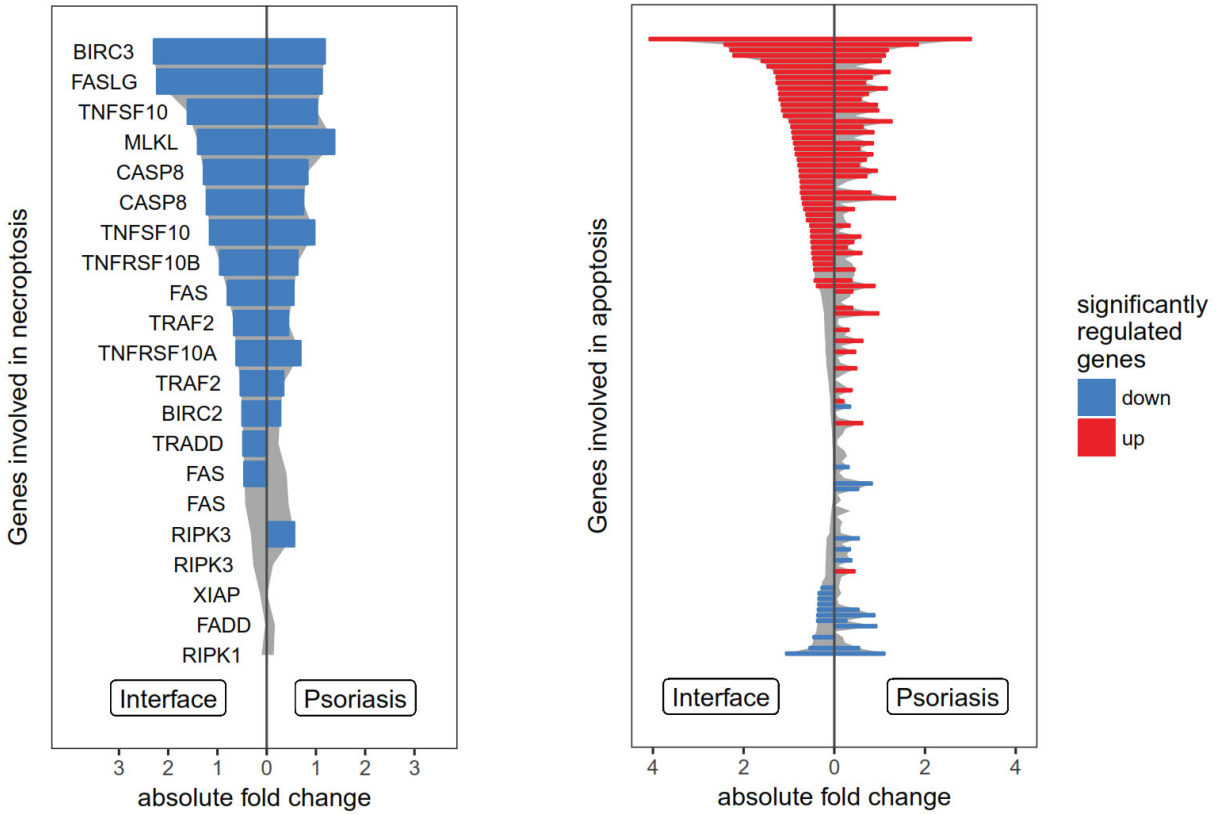

Supplementary Figure S2 Correlation analysis of histological attributes